



Controls on the terrigenous fractions in Early Kimmeridgian shallow-water carbonate deposits in Southern Iberia

Rute Coimbra¹  · Federico Olóriz² · Fernando Rocha¹

Received: 5 April 2024 / Accepted: 8 July 2024
© The Author(s) 2024

Abstract

Two Kimmeridgian shallow-marine carbonate successions (mid-shelf), sharing a similar paleoclimatic framework (climatic zone), were previously explored using carbonate chemostratigraphy. Before, the goal was to detect signals related to paleo-platform bottom physiography, degree of connection with oceanic waters and overall circulation patterns. In this contribution, complementary bulk mineralogical composition and clay mineral fractions are investigated to contrast and complement previous information, aiming for a more complete overview of continent-ocean dynamics along shallow-carbonate platforms of southern Iberia. The goal is now to explore complex patterns of continental influence along proximal settings and their relative spatial distribution across differentiated settings without relevant difference in paleolatitude. The choice of both stratigraphic sections is based on this distinctness: Rocha Poço (Algarve Basin, Portugal) represents a more restricted and relatively proximal setting, in contrast to Puerto Lorente (South Iberian Paleomargin, S Spain) placed at a relatively more open and probably distal shallow-water context. Accordingly, quartz content was higher at Rocha Poço, especially at the lower siliciclastic interval of this section. Quartz contribution fades out at Puerto Lorente, where it was mainly controlled by short-lived terrigenous pulses. Clay mineral assemblages also differed, being more varied (smectite, illite and traces of kaolinite) and abundant at Rocha Poço, and generally leaner at Puerto Lorente. At the latter site, terrigenous pulses do not contribute to clay mineral abundance, only showing abundant illite at the topmost horizons. New information retrieved from mineralogical data provided evidence on depositional contrasts resulting from local differences in platform configuration, allowing a better understanding of mechanisms controlling the terrigenous fraction in the shallow-water carbonates analyzed.

Keywords Paleoenvironmental events · Kimmeridgian · Shallow-water carbonates · Mineralogy · X-ray diffraction

Resumen

Dos sucesiones de sedimentos marinos carbonatados de aguas someras (plataforma media), en un contexto climático similar (zona climática), fueron previamente investigadas mediante el análisis quimioestratigráfico de las fases carbonatadas. El objetivo entonces fue la identificación de señales relacionadas con la fisiografía de las plataformas, el grado de conexión con las aguas oceánicas y los patrones generales de circulación de las corrientes marinas. En esta contribución se investiga la composición mineralógica complementaria de la muestra total y los minerales de la fracción arcillosa con el objetivo de contrastar y complementar la información previa, así como para obtener una visión más completa de la dinámica de la interacción continente-océano en plataformas carbonatadas poco profundas y distantes en el sur de Iberia. En detalle, se persigue la caracterización de los patrones complejos de la influencia continental en áreas epicontinentales, neríticas proximales, así como su distribución espacial relativa en emplazamientos distanciados, pero sin diferencias notables en paleolatitud. La elección de los perfiles está basada en el contraste de sus diferencias: El perfil de Rocha Poço representa un emplazamiento marino relativamente proximal y comparativamente confinado, mientras el perfil de Puerto Lorente muestra rasgos de un

✉ Rute Coimbra
rcoimbra@ua.pt

¹ GeoBioTec, Department of Geosciences, University of Aveiro, Campus de Santiago, 3810-193 Aveiro, Portugal

² RNM178 Research Group, Department of Stratigraphy and Paleontology, University of Granada, Granada, Spain

contexto marino más abierto y probablemente algo más distal. En consecuencia, el contenido en cuarzo registrado en Rocha Poço fue más alto, especialmente en el intervalo siliciclástico basal, mientras que en Puerto Lorente muestra estrecha relación con eventos de aportes terrígenos. Las asociaciones minerales de la fracción arcilla también muestran diferencias. Son más diversificadas y abundantes en Rocha Poço (esmectita, illita y trazas de caolinita), mientras que en Puerto Lorente los eventos de aportes terrígenos no incrementaron la fracción arcilla, que solo muestra illita abundante en los horizontes más jóvenes. La nueva información obtenida de la fracción arcilla evidencia contrastes en las condiciones de depósito que resultan de diferencias locales en la configuración de las plataformas, lo que ha permitido una mejor comprensión de los procesos que controlaron la fracción terrígena en los carbonatos de aguas poco profundas analizados

Palabras clave Eventos paleoambientales · Kimmeridgiense · Carbonatos someros · Mineralogía · Difracción de rayos X

1 Introduction

1.1 Global climate during early Kimmeridgian times and a related context for the South Iberian Paleomargin

The Late Jurassic climate experienced shift to drier conditions with respect to previous Jurassic times (Abbinck et al., 2001; Boulila et al., 2022), was globally warm, with relatively low latitudinal thermal gradients, reduced and no permanent ice caps at high-latitude (Moore et al., 1992a; Valdes & Sellwod, 1992; Rees et al., 2000; Rais, 2007), while a zonally differentiated climate included a Inter Tropical Convergence Zone (ITCZ) larger than today and with irregular layout. At a global scale, the environmental dynamics forced by monsoonal winds would be more relevant than that derived from regional/local winds, especially for large land masses (Parrish et al., 1982; Hallam, 1984; Chandler et al., 1992; Weissert & Mohr, 1996), but conditioned by the reduced thermal gradient. In general, biocalcification was favored under “normal” trophic conditions (Weissert & Erba, 2004), while dysoxic waters have been modeled for westernmost Tethys during Late Jurassic and earliest Cretaceous times (Scotese & Moore, 2014a). Kimmeridgian times were comparatively “cooler” (cool greenhouse conditions s. Holz, 2015), showing increasing temperature during the major transgressive interval of the Early Kimmeridgian (Dercourt et al., 1994; Dera et al., 2011) even in Suboreal areas (Wierzbowski et al., 2013). High-frequency temperature fluctuations have been identified in Early Kimmeridgian marl-limestone couplets from SE France and interpreted as DO analogous rhythms of low latitude (Boulila et al., 2022).

Overall, climatic models show Iberia between 20–30°N and 10–15°E, exposed to easterlies far from storm and monsoon tracks (Ross et al., 1992: subtropical cyclone storms 10°N–10°S in summer and 20°N in winter; Colombié et al., 2018 for northwards winter storms but potential influence of tropical cyclones), under low precipitation (Moore et al., 1992b), and with negligible relief in terms of the paleotopographic ranges modeled. The SE Iberia faced water masses with sea surface temperature ca. 30°C (Moore et al., 1992b) and under rather intricate marine currents (Moore et al., 1992a, 1992b showing dominant easterlies

vs. westerlies when topography is approached, respectively; Demko & Parrish, 1998; Scotese & Moore, 2014a, 2014b) resulting from irregular sea bottoms across the epiocceanic fringe, including hypothetical bidirectional flows (Challinor & Hikuroa, 2007 based on Parrish, 1992). SE Iberia was relatively close to areas of precipitation < evaporation centered in NW Africa during summer and showing annual net evaporation in winter (Moore et al., 1992b; Ross et al., 1992; Weissert & Mohr, 1996). There is no evidence of relevant inland relieves in southern Iberia (within the lower range of models by Moore et al., 1992b). Hence, amongst regions without huge orography and close to low-latitude large warm water masses (surface waters > 27 °C; Moore et al., 1992a), southern Iberia would experience ocean stabilizing modulations of temperature (Moore et al., 1992b; Rees et al., 2000). –i.e., a climatic context prone to small fluctuations (the maritime greenhouse effect in Kyessling et al., 1999) aside from those potentially related to tectono-eustatic events.

During the Late Jurassic, Iberia has been interpreted to be placed within an interval of latitude between 20°N and slightly above 30°N (Fig. 1A), close to the connection of the west Tethys with the Hispanic Corridor growing through the Central N. Atlantic Basin (Ross et al., 1992; Decourt et al., 1994; Ford & Golonka, 2003; Vrielynck & Bouysse, 2003; Ziegler et al., 2003; Rais, 2007; Brigaud et al., 2008; Schettino & Turco, 2009; Boulila et al., 2022). During the Late Jurassic, the S-SE paleomargin of Iberia was structured as an epicontinental shelf system dominated by a ramp model with locally variable abrupt shelf-breaks (the Prebetic and lateral equivalents), which connected with the epiocceanic environment southwards (the Subbetic; synthetic view in Olóriz, 2002, and references therein). In the latter, bottom physiography was irregular according to trends of finally arranged SW–NE lineaments of epiocceanic swells and troughs. North-to-south, landwards-to-seawards, swell ranges are the External Subbetic, the Internal Subbetic, and lateral equivalents. North-to-south troughs are the Intermediate Units, the Median Subbetic Zone, and lateral equivalents, and the southernmost basin separated by oceanic crust from the also physiographically complex Alboran Domain. The later here refers to epiocceanic-oceanic environments respectively (Olóriz, 2000 and references therein), southwards from the

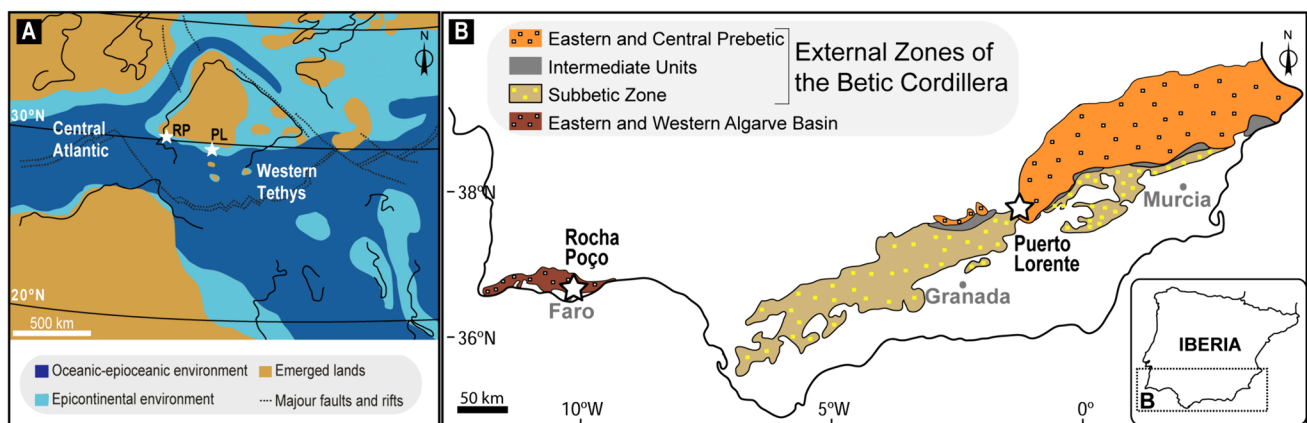


Fig. 1 Geographical location of the studied sections (**stars** indicate locations of the studied sections). **A** Late Jurassic paleogeographic reconstruction of western and central Tethyan realm. Plate tectonic setting from Stampfli and Borel (2002) and depositional environ-

ments after Thierry et al. (2000); **B** Regional distribution of major geological units along the Betic Cordillera (modified from García-Hernández et al., 1980)

External zones of the Betic Cordillera at its western extreme, merging with equivalent environments southwards from the Algarve. A 5–10 km wide huge pile of volcanic rocks that represents the Median Subbetic Volcanic Ridge (Mid-Subbetic Volcanic Ridge of at least 700 m high during the Late Jurassic; Comas et al., 1986), was active in the central part of the Median Subbetic Trough partially forcing subdivision of this trough in a southern and a northern arm, within a volcanic strip across ca. 300 km. The latter figure especially applies when pillow lavas 160 Ma old, eastern from the central sector of the Median Subbetic (Fliert et al., 1979) are considered. These represent the oldest Upper Jurassic pillow lavas reported, giving an Early Oxfordian age according to present revisions of absolute ages (GTS, 2020) and, hence, older than those of Early Tithonian age reported by Comas et al. (1986) from the Central Subbetic.

In the central sector of the Betic Cordillera epicontinental shelves (the Prebetic Zone and lateral equivalents) freely connected with the Tethyan epioceanic environment (the Subbetic Zone, lateral equivalents and southernmost basins) through shelf-breaks facing the adjacent troughs—the Intermediate Units and lateral equivalents.

A wider palaeogeographic context S-SE Iberian palaeomargin shows the alluded Alboran Domain as part of a complex frame of epioceanic-oceanic troughs, with variable continuity throughout the Iberian and north African distal palaeomargins, resulting from extensional to hyper-extensional regimes during the Jurassic, with a special pulse during the Late Jurassic-Early Cretaceous. Major epioceanic-oceanic passages were related to the West Ligurian or Betic arm and the East Ligurian-Maghrebian arm of the western Tethys, both merging into the transtensional zone connecting westward to the growing Hispanic Corridor forced by the evolution of the Central North Atlantic Basin.

These two major oceanic arms contoured at least one main microcontinent, block, plate, or microplate, first named as the Alboran subplate and the mesomediterranean subplate (Andrieux et al., 1971; Durand-Delga & Fontboté, 1980), and then the ALKAPECA palaeogeographic Domain (Boillin et al., 1986), assumedly fragmented during Cenozoic times. The above mentioned Alboran Domain refers to the western extreme of such a microcontinent, whose interpretations are debated up today (Angrand & Mouthereau, 2021; Moragues et al., 2021; and references therein), but without palaeoenvironmental incidence for our contribution.

In the area investigated in the Algarve (southern Portugal, SW Iberia), the epicontinental shelf system included a huge carbonate shelf westward, and distal shallow carbonate banks identified by ocean drilling southwards (Boillot et al., 1974; Baldy et al., 1977; Mougénot et al., 1979, among others) labelled the southern sector of the Algarve Basin by Marques and Olóriz (1989a, 1989b). Offshore wells and outcrops westwards to the growing central North Atlantic show that carbonates with common dolomitization dominated deposition during Kimmeridgian times (Rocha, 1976; Pereira, 2013). In the Alentejo Basin, Lower Kimmeridgian deposits included corals and low diversified dinocysts from partly confined comparatively small basins (lagoons and shallow waters) where pollen and spores were more abundant than marine foraminifera (Borges et al., 2011). Reef growth was assumed diverse across ramp, basin, and slope environments during Kimmeridgian times (Kiessling et al., 1999).

Eastwards from the huge carbonate shelf and northwards from the distal shallow carbonate banks, a depression formed the northern sector of the Algarve Basin or Central-Eastern Algarve Basin (Marques & Olóriz, 1989a, 1989b). This was a rather restricted neritic environment confined westwards

and southwards by shallow carbonates, and northwards by Hercynian lands of SW Iberia, but it was devoid of raised bottoms eastward that would hinder an open connection of bottom waters from the Central-Eastern Algarve Basin with Tethyan oceanic waters. This context agrees with the eastwards increasing in fine clastics vs. carbonates in the southern offshore wells mentioned. Hence, the expected direct transportation of clays from the Central-Eastern Algarve Basin southwards to the ocean was distorted and/or disabled.

1.2 Overview and current interest of comparing deposition in proximal settings from Southern Iberia: a lower Kimmeridgian example

Unravelling paleoenvironmental conditions from ancient carbonate archives is a challenging task. In order to explore an innovative and more holistic approach, the Late Jurassic carbonate record from the southern paleomargin of Iberia has been under investigation. Under strict biostratigraphic control, a selection of several stratigraphic sections along Southern Portugal, Southern Spain and the Majorca Island configured a proximal to distal transect, covering a wide variety of depositional environments from epicontinental to epiocanic and providing a unique overview of the sedimentary dynamics in time and space (Coimbra, 2011).

The most relevant outcomes from both the Rocha Poço and Puerto Lorente sections, here under scope, are briefly summarized to place the current research in a wider context. Particular carbon and oxygen isotope composition of the epicontinental Rocha Poço section were explored in Coimbra et al. (2014). Of particular relevance, it allowed to identify a syn-depositional forcing under the local influence of non-marine water on the middle shelf (mixing of marine and freshwater primary signals), coupled with a later diagenetic component related to the presence of interstitial fluids (freshwater/brackish) during burial in the lowermost more porous, permeable silty facies. As for the more spongiolithic facies, active organic matter decay related to significant microbialite occurrence agrees with slight differences in C and O-isotope composition, denoting decreasing continental influence and a differentiated diagenetic pathway when compared to typical Ammonitico Rosso facies from the epiocanic fringe, whilst maintaining a comparable stratigraphic trend regarding Lower Kimmeridgian epiocanic records (Coimbra et al., 2015).

Apart from the described complex C and O-isotope record, elemental abundance throughout the Rocha Poço section was equally enlightening when compared to coeval epiocanic signals (Coimbra et al., 2015). Major differences in elemental record related to a depositional setting including geochemically different nearshore waters, even more relevant for intervals of higher continental influence. A persistent influx from continental sources was detected,

coupled with a marked influence of active reefal growth in the vicinity of this area.

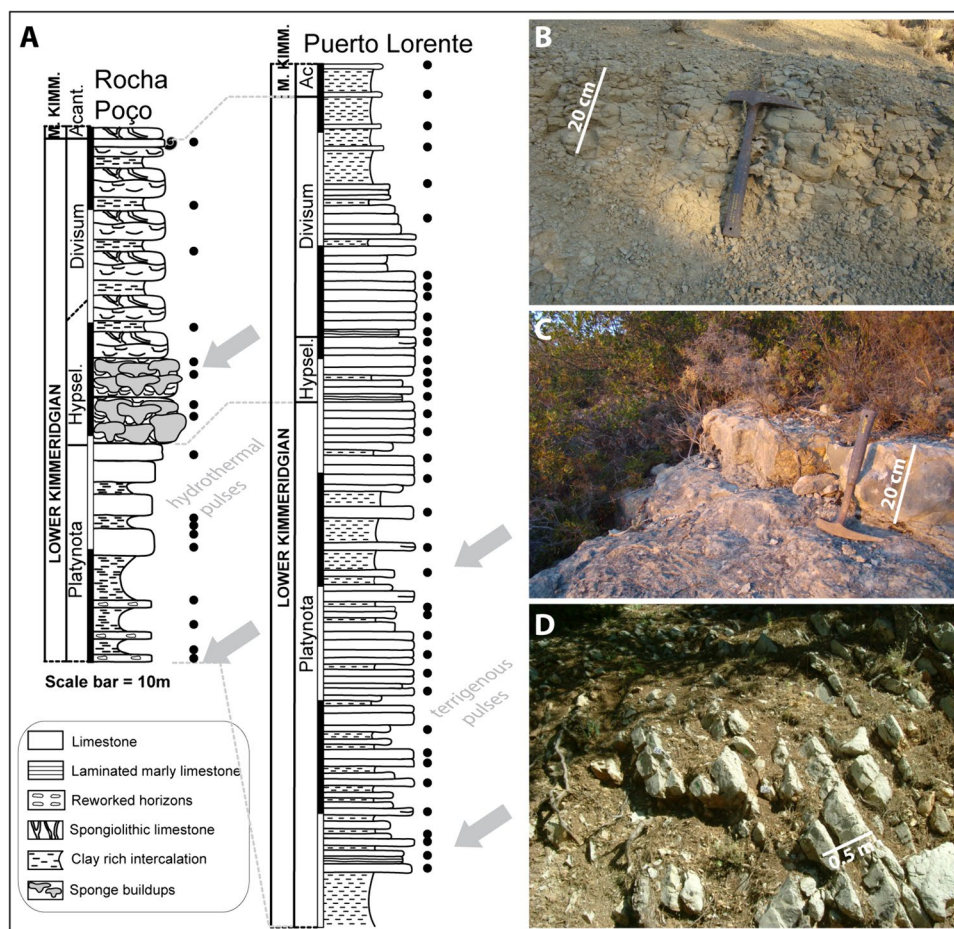
Due to the highly informative nature and singular relevance of the geochemical record at the epicontinental Rocha Poço section, this section was later compared with the probably more distal, but equally shallow-water section outcropping at Puerto Lorente (External Prebetic) to test the sensitivity and reliability of carbonate chemostratigraphy (Coimbra et al., 2019). Maximum impact of continental influence was evidenced at the Rocha Poço section, fading out along the mixed carbonate-fine siliciclastic rhythmic deposition in the more open Puerto Lorente section. Local forcing by upwelling in the surroundings of a coral fringe was deduced for the Rocha Poço section, and the geochemical signature of hydrothermal influence was differentiated from terrigenous pulses. Furthermore, the influence of tectonic activity affecting nearshore/coastal water masses was depicted in both sections.

After an in-depth geochemical characterization of the carbonate fraction of the selected sections in Southern Iberia, the challenge of complementing this information with independent mineralogical (bulk and clay fraction) data brings new light into previously studied materials. In this way, the goal is to provide complementary evidence to refine interpretations on the controls on terrigenous fraction distribution patterns in differentiated shallow-water settings along Southern Iberia and the forcing paleoenvironmental dynamics. The applied approach combines several tools that were designed to be applicable to a wide range of materials and fields of research, resulting in cost-effective and/or time-saving solutions that optimize data visualization and perception.

2 Studied sections, geological and paleoenvironmental context

The interpretation of geological and paleoenvironmental evolutions of the selected two epicontinental sections is approached on the basis of both favorable outcrop conditions and a tight biostratigraphic control (Marques, 1983; Marques & Olóriz, 1989b, 1992; Olóriz & Rodríguez-Tovar, 1993a, 1993b, Coimbra et al., 2019; Figs. 1 and 2), here improved punctually. The Rocha Poço section represents epicontinental deposition along the SW Iberian paleomargin, in the eastern Algarve Sub-basin in southern Portugal (Fig. 1A and B). Irregular bottoms in the latter resulted from N-S strike-slip faults and extensional tectonics E-W combined with salt movements (Manupella et al., 1988). Eco-sedimentary conditions in the eastern and western sub-basins differed throughout the Jurassic due to persistent shallow carbonate shelf-system conditions westwards. Offshore boreholes identified southern carbonate shelf or blocks that seem to represent the external edge of epicontinental conditions

Fig. 2 Stratigraphic representation of comparable time intervals for the Rocha Poço and Puerto Lorente sections. **A** Lithofacies variability and lateral correlation among sections. **Dots** indicate stratigraphic sampling density; **arrows** indicate pulses identified in previous works (terrigenous and hydrothermals, Coimbra et al., 2015, 2019). **B to D** Field views representative of the siliciclastic interval at the lowermost portion of the Rocha Poço section, the spongiolithic limestone at Rocha Poço and the typical succession of limestone beds at Puerto Lorente section (supplementary field photos can be found in Coimbra et al., 2019). Biostratigraphy at the ammonite biozone level on the left

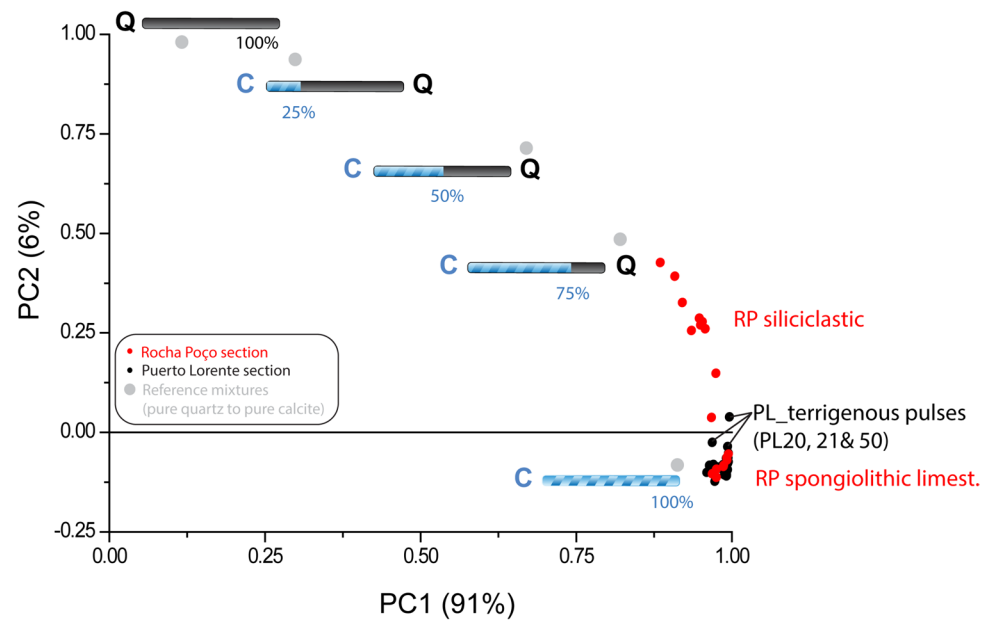


(Marques & Olóriz, 1989a), or part of a more complex margin north of the Newfoundland-Gibraltar Fault Zone, being southwards open-sea Tethyan oceanic-epioceanic waters. In the restricted mid-neritic shelf of the eastern Algarve Subbasin irregular bottoms favored local developments of bioherms with sponges and/or corals (Marques, 1985; Ramalho, 1985; Rosendhal, 1985; Leinfelder, 1993), and changes in facies and stratigraphic discontinuities are common throughout the Oxfordian and the Lower Kimmeridgian (Marques & Olóriz, 1989b). The previous arguments point towards paleoenvironmental variability, including nutrients and bottom currents amongst others.

Coimbra et al. (2019) provided a detailed analysis of environmental conditions favoring spongiolithic facies and sponge buildups. Some complementary observations apply: Relative eutrophication would be locally reinforced by upwelling rather than continental runoff. Upwelling events on a mid-shelf will force increasing nutrients and relative lowering of sea-water temperature, phytoplankton blooms and the related food-web reducing water transparency, and the occurrence of heterotrophic massive sponges dominant in carbonate-fine siliciclastic sediments as a rapid response with notable growth, which would be especially

fueled in relatively enclosed sites or in proximal sites (Hallock & Schlager, 1986; Birkeland, 1987; Wilkinson, 1987; Wood, 1993, 1998). The growth of microbial communities and suspension-feeding metazoans would benefit mixotrophic sponges towards heterotrophy based on dissolved and particulate organic matter exported during pulses of higher productivity, and mesotrophic conditions (see Olóriz et al., 2003, 2006 and references therein for supplementary interpretation of Oxfordian sponge buildups and spongiolithic limestones westward in the Prebetic), under persistent dominance of mixed deposition of carbonates and fine clastics while precipitation of inorganic cement increased (Wilkinson, 1987; Wood, 1998). Amongst the microfossils identified by Coimbra et al. (2019), the combined occurrence of *Tubiphytes* s. Flügel (2010) and remains of hexactinellid spicules confirms analogy with well-known Late Jurassic sponge-*Tubiphytes* reefs (Flügel, 2010; note that Mesozoic *Tubiphytes* have been referred as *Crescentiella* n. gen. proposed by Senowbari-Daryan et al., 2008 to separate from Paleozoic *Tubiphytes* based on the structure of the symbiotic cyanobacterial encrustments on “hard bio-substrates”); remains of hexactinellid spicules and the meagre occurrence of calcified zoospores of, or single-celled, planktic algae

Fig. 3 Results of Principal Component Analysis (PCA) of bulk mineralogical XRD spectra, compared to pure quartz and calcite compositions, as well intermediate progressive increments in calcite (Q: quartz; C: calcite)



(*Globochates*), together with absence of *Sacoccoma*, are compatible with outer-middle shelf conditions. In addition, reworked miliolids and fine- and locally medium-size quartz without identifiable hummocky stratification also points to a mainly low depositional scenario across the outer-middle shelf, dominated by wackestones and local sponge buildups on low relieves related to salts movements.

Inner-shelf conditions favoring homogenized carbonate sedimentation occurred during the mid-Late Kimmeridgian before the peak regression of latest Jurassic-earliest Cretaceous times (Marques, 1985; Manupella et al., 1988; Marques & Olóriz, 1989b), in accordance with that revealed in the epicontinental shelf system across southern Iberia (Marques et al., 1991; Pereira, 2013; and references therein).

The Rocha Poço section of reference shows two well-marked stratigraphic intervals (Fig. 2A): 20 m of silty limestones and marls in the lower part, underlying to 28 m beginning with local buildups followed by spongiolithic limestones and related facies (Peral and Cerro da Cabeça Formations) (Marques, 1985; Ramalho, 1988; Coimbra et al., 2014). At the lower 8 m of the spongiolithic interval huge development of sponge buildups occurs (Fig. 3B). Without latitudinal difference between the Algarve Basin and the central Prebetic, distinctive tectonics was active during the Early Kimmeridgian. Salt tectonics in the eastern Algarve Sub-basin forced high bottom irregularities, while bottom instability and differential subsidence were registered in the mixed carbonate-siliclastic rhythmites in the Prebetic, where outer-shelf areas corresponding to the comparatively distal Internal Prebetic during the Platynota Chron experienced local synsedimentary sliding (Olóriz & Rodríguez-Tovar, 1998).

In the Cazorla sector in the External Prebetic, the Puerto Lorente section (Figs. 1 and 2) shows Kimmeridgian deposits belonging to mid-shelf eco-sedimentary conditions within the epicontinental shelf-system of the Betic Cordillera (Fig. 1), without clear possibility for a more precise interpretation about its precise paleogeographic setting. Overall, the External Prebetic was a low energy, enlarged eastward shelf showing distally steepened ramp whose outer part corresponds to the Internal Prebetic, which represent outer-shelf environments south to south-eastward, shelf-break and steep slope separated epicontinental and epioceanic waters and, hence, its eco-sedimentary domains. The latter indicated by the northernmost, adjacent trough –the Intermediate Units– and then by the complex of NE-SW swells-and-troughs belonging to the front of the allochthonous Subbetic (Olóriz, 2002 and references therein for extended treatment). The Puerto Lorente section represents deposition on a comparatively raised bottom within the neritic zone, which registered condensed, hiatal deposition during Oxfordian and oldest Kimmeridgian times (Bimamatum pro parte and Planula chrons). The combined record of *Sutneria galar* and *S. platynota* in a ferruginized surface on top of the Upper Oxfordian succession indicates condensation higher than the assumed for within-habitat time-averaging (Olóriz, 2000). Therefore, it implicates hiatal deposition and biostratigraphic condensation, being the interpreted age for the ferruginized surface (“hardground” or hardground of AA) to be determined by the youngest fossil registered (*Sutneria platynota* according to Olóriz & Rodríguez-Tovar, 1993a, 1993b). Marques et al. (1991) envisaged probable hiatuses related to the ferruginized surface, affecting unknown horizons of the Planula and Platynota zones, while the non-record of *Sutneria platynota* type

A Schairer (1970) in Olóriz and Rodríguez-Tovar (1993a) indicates absence of at least unknown horizons belonging to the lower part of the Platynota Zone, which agrees with the lack of complex ribbing in ataxioceratin ammonites from the lower part of the overlying marly interval. All of this allows the improving of the interpretation made by Olóriz and Rodríguez-Tovar (1998), assuming morphotype correlation of Franconian and Prebetic *Sutneria platynota*. Difficulties found by Olóriz and Rodríguez-Tovar (1998) for the biostratigraphic recognition of hiatuses in the uppermost Oxfordian are assumed given the information available at present. Overlies a three meter-thick interval of siliciclastics useful for correlation at regional scale (Fig. 2), thus revealing Early Kimmeridgian instability at the lowermost Platynota Zone. It corresponds to the local record of a tectonic pulse preceding abrupt increases in subsidence in the Iberian subplate (Acosta, 1989; Olóriz et al., 2012, and references therein), as well as in northwest Africa and Submediterranean Europe (Marques et al., 1991; Leinfelder, 1993; Aurell et al., 2002; Colombié et al., 2014). The following 100 m of marly and silty limestone rhythmite (Lorente Fm.; Pendas, 1971), were deposited under warm climate with slight changes in the precipitation-evaporation ratios, as indicated by clay mineralogy (López-Galindo et al., 1994). Olóriz and Rodríguez-Tovar (1998) assumed a subtropical, maybe seasonal, climate based on mineralogical analyses by López-Galindo et al. (1991) and Rodríguez-Tovar (1993, and references therein). The stratal patterns point to tectono-eustatic forcing on relatively shallow sea bottoms, while background control on sedimentation in the middle part was mainly due to orbital forcing, long- and short-term eccentricity and precession rather than obliquity cycles; interactions with eustasy occurred in the upper part of the section (Olóriz et al., 1992; Olóriz & Rodríguez-Tovar, 1998). López-Galindo et al. (1991) first identified the influence of bottom topography on clay minerals distribution.

The stratigraphic correlation between the two selected sections at Rocha Poço (S. Portugal) and Puerto Lorente (S-SE Spain) was based on ammonite biostratigraphy at the biozone and subbiozone level (Marques, 1983; Marques & Olóriz, 1989a, 1992; Olóriz & Rodríguez-Tovar, 1993a, 1993b), here refined (Fig. 2B). Guide-fossils in successive ammonite assemblages at the biozone level are *Sutneria platynota*, *Crussoliceras divisum*, *Orthaspidoceras uhlandi* and *Taramelliceras compsum*.

Coimbra et al. (2019) investigated geochemical signals related to paleoplatform bottom physiography, degree of connection with oceanic waters and overall circulation patterns in the two Kimmeridgian shallow-marine carbonate sections of interest. The Fe and Mn coupling was evident in both sections, revealing overall terrigenous inputs

along both epicontinental areas, being related elemental supply more significant for the Rocha Poço section, especially in the lowermost siliciclastic interval (Fig. 2A and C). Peaks in siliciclastic input denote sharp transitions probably related to local tectonic pulses rather than reactivations of the hydrological cycle, agreeing thus with major geochemical forcing due to hydrothermal contribution, i.e., syndepositional submarine volcanic activity (identified pulses indicated in Fig. 2A). This activity is typically characterized by sharp Mn input without major Fe changes, among others such as related hydrothermal discharges through fracture zones in the highly structured SW Iberia paleomargin and related oceanic-epioceanic areas close to the growing connection to the Hispanic Corridor. In summary, differential forcing in processes affecting the South Iberian paleomargin during early Kimmeridgian times, including a variable degree of continental influence fading out in less restricted settings.

To provide an in-depth overview of these patterns, mineralogical analysis was performed to contrast and complement previous information, aiming for a more complete overview of the influence of the continent-ocean dynamics along shallow mixed carbonate-siliciclastic platforms. Hence, using mineralogical data will provide new evidence on depositional contrasts resulting from local differences in platform physiography, among others, allowing a better understanding of the mechanisms controlling the terrigenous fraction in shallow-water carbonates.

3 Materials and methods

A total of 55 samples (18 from Rocha Poço; 37 from Puerto Lorente) were selected, including a variety of lithofacies ranging from carbonate-rich facies at Puerto Lorente, carbonate-rich spongiolithic facies at Rocha Poço and samples with lower carbonate content corresponding to the siliciclastic interval at Rocha Poço. Bulk mineralogical composition was determined by X-ray diffraction (XRD) with Cu-K α radiation, carried out on non-oriented mounts of previously grinded samples, using a Malvern Panalytical Phillips X'Pert PW3040/60 equipped with X'Pert 2.0 and Profit software at the facilities of the Department of Geosciences, University of Aveiro, Portugal. Scans were run between 4 and 65° 2 θ for bulk (non-decarbonated) samples and between 2 and 20° 2 θ of oriented powder mounts of fine (clay) fractions for clay mineral identification. Clay mineral identification was obtained after decarbonation. Decarbonation protocol followed the guidelines provided by Coimbra et al. (2021), using 2N acetic acid solution at 50 °C for one

hour reaction time. Scans were run between 2 and 20° 2θ on oriented powder mounts for fine (clay) fractions in the air-dry state (natural sample), as well as with glycerol saturation and heat treatment at 500 °C. After decarbonation, the insoluble residue was also measured to access the mineral assemblage not destroyed by this procedure. Peak identification was performed manually (following Brindley & Brown, 1980) and abundance is compared based on peak intensity of each mineral, as highlighted in Coimbra et al. (2022).

Statistical analysis of XRD results (here Principal Component Analysis- PCA) was performed to compare the obtained bulk mineralogy diffractograms with standards of endmember composition of 100% quartz to 100% calcite, also including stepwise increment in calcite content (25%, 50%, 75%). PCA was favored for highlighting similarities and differences in the patterns detected (see Wold et al., 1987 for detailed description) since this reduction technique includes several samples within one single diagram, thus providing a very intuitive visual output. A total of 60 diffractograms were processed using PCA in only a few minutes, including 5 standard composition samples and the 55 diffractograms comprising the focus of the experimental essay. This approach allows a fast overview of sample variability, bypassing successive interpretations of spectra.

Additionally, a customised display of raw XRD data was performed following Coimbra et al. (2022), generating 3D models to provide a clear overview of the complex mineralogical dataset obtained, also allowing an expedite comparison between both studied sections.

4 Results

4.1 PCA analysis of diffractogram spectra

Principal component scores indicated the relative contribution of each sample for the respective principal component. When compared to standard composition of pure quartz and calcite, as well as mixtures of both at 25% increment of calcite, samples from Rocha Poço and Puerto Lorente fall within the compositional range of 25% to absent quartz (Fig. 3), also evidencing lower carbonate content in the siliciclastic interval at Rocha Poço section when compared to terrigenous intervals at Puerto Lorente section. Specifically, samples denoting higher abundance of quartz correspond to the siliciclastic interval representing the lower portion of the Rocha Poço section (Fig. 2A, C), decrease towards lower contents for samples corresponding to previously identified terrigenous pulses at

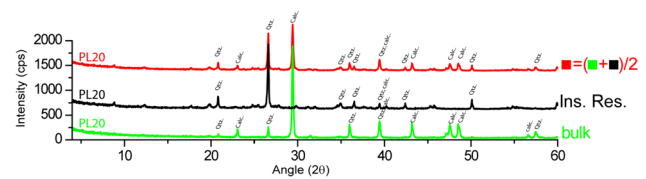


Fig. 4 Example of the mineralogical approach applied to the studied sections (here XRD spectra from sample PL20 from the base of the Puerto Lorente section). Note that including bulk mineralogy along with insoluble residue (red) results in a more representative characterization of the materials under scope (see text for details)

Puerto Lorente (Fig. 2A). In contrast, samples belonging to the spongiolithic upper portion of Rocha Poço and most Puerto Lorente samples fall within the PCA space enclosing to samples denoting high calcite content.

4.2 3D models of mineralogical assemblage

Sample processing as described in Sect. 3 results in two sets of diffractograms: bulk mineralogy and the insoluble residue measured after decarbonation (example in Fig. 4). Due to the carbonate nature of the samples, the bulk mineralogy spectrum is largely dominated by the intensity of calcite peaks, obscuring other minerals. After decarbonation this peak is eliminated, and the remaining mineralogical assemblage can be fully appreciated. In order to highlight the contribution of the complete mineralogical assemblage, both spectra were summed and divided by two, the later step serving to reduce exaggeration in peak intensity (Fig. 4). The resulting spectra were expanded under 3D model computation.

For the more restricted setting at Rocha Poço (Fig. 5A), bulk mineralogy results revealed a stratigraphic trend of abundant quartz still reaching this area, but decreasing as calcite deposition dominated the upper portion of the sedimentary record. In contrast, for the comparatively open location at Puerto Lorente, stratigraphic abundance of quartz is very restricted, punctual (Fig. 6A), verified mainly as sharp and prominent peaks, coinciding with previously identified pulses of continental influx (Fig. 2).

The clay fraction also provided very distinct patterns at each of the sections investigated. The more restricted and relatively proximal setting at Rocha Poço revealed a significantly higher abundance of smectite and illite when compared to the more open and relatively distal site of Puerto Lorente, and this is especially relevant at the lowermost portion of this section (Fig. 5B). Limited occurrence of kaolinite is also characteristic for this relatively proximal Rocha Poço site. At the more open and probably relatively distal site (Puerto Lorente section), clay mineral abundance was overall lower, comprised mainly by illite and (irregular) illite/smectite, with small amounts

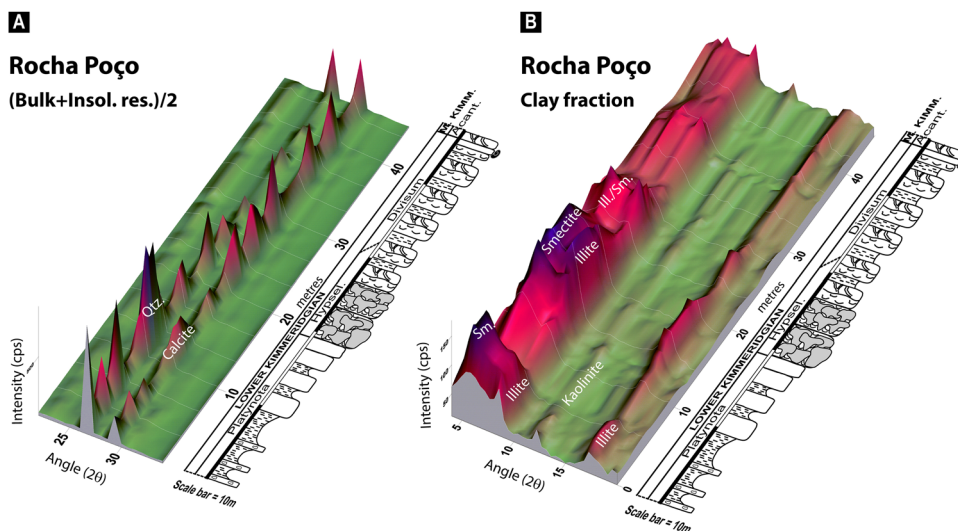


Fig. 5. 3D modelling of raw XDR intensity data for the Rocha Poço section, highlighting the most significant results (lithology as in Fig. 2A). **A** Bulk mineralogy showing stratigraphic variation of quartz and calcite. Peaks with highest amplitude (primary peaks) are identified as calcite, quartz based on peak position. **B** Clay fraction

3D model. In all models, peak width is exactly as obtained from XRD measurements. Secondary/tertiary less intense peaks of these same minerals are not identified here for reasons of simplicity (except for illite in the clay fraction spectra)

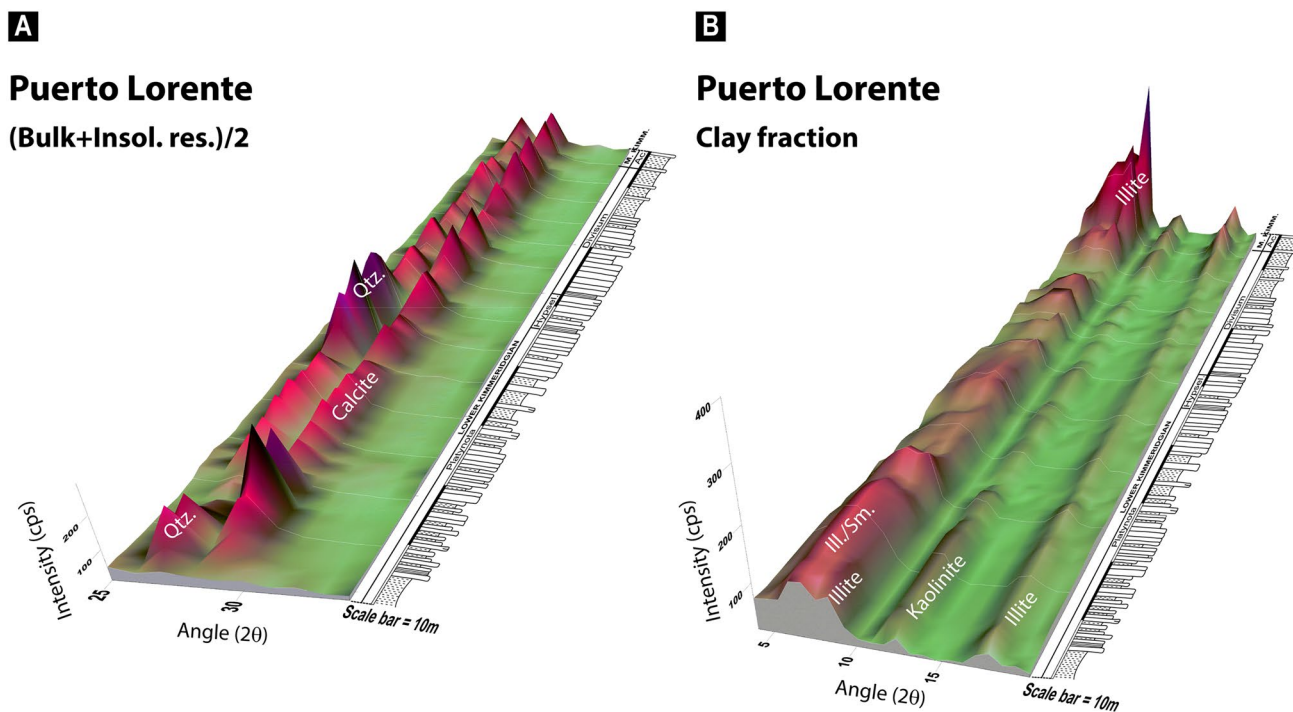


Fig. 6. 3D modelling of raw XDR intensity data for the Puerto Lorente section, highlighting the most relevant results (lithology as in Fig. 2A). **A** Bulk mineralogy showing stratigraphic variation of quartz and calcite. Peaks with highest amplitude (primary peaks) are identified as calcite and quartz based on peak position. **B** Clay frac-

tion 3D model. Peak width is exactly as obtained from XRD measurements. Secondary/tertiary less intense peaks of these same minerals are not identified here for reasons of simplicity (except for illite in the clay fraction spectra)

of kaolinite (Fig. 6B). At the lowermost portion of the Puerto Lorente section, a slightly higher contribution of

illite and interstratified illite/smectite is verified along with small amounts of kaolinite, decreasing towards the

mid-portion of this section. A conspicuous increase in illite and illite/smectite is observed towards the top of this section, a trait that is not recognized along any other bulk mineralogical nor geochemical proxies indicating elevated terrigenous input (Figs. 2 and 6) based on the assumption of low diagenetic imprint (see below).

5 Interpretation and discussion

5.1 Diagenetic considerations on clay mineral assemblages

When interpreting clay mineral associations extracted from ancient sedimentary records, factors as sedimentary reworking, diagenesis mainly through burial derived temperature and tectonics (Raucsik & Merényi, 2000; Thiry, 2000; Ruffel et al., 2002; Arostegui et al., 2006; Godet et al., 2008; Lanson et al., 2009; Coimbra et al., 2021; Boulila et al., 2022) and/or authigenesis may alter the primary assemblage of clays, thus obscuring their original paleoclimatic signal. Possible indicators of fair preservation of clay mineral assemblages include records of abundant smectite along with variations in smectite/illite ratios in marls-limestone couplets and preference of illite in marly levels (Boulila et al., 2022); persistent records of opposite values amongst key clay minerals (Deconinck et al., 1996); high smectite contents indicating relatively low burial-temperature and diagenesis (Godet et al., 2008; Deconinck et al., 2019); coherence with geochemical records (Coimbra et al., 2021); distribution of clay species according to sea-levels, currents and/or winds (Raucsik & Merényi, 2000; Hattem et al., 2017). On the assumption that significant alteration can be ruled out, several clay species can be successfully used as indicators of paleoclimatic conditions for the Mesozoic period (Raucsik & Merényi, 2000; Ruffell et al., 2002; Schnyder et al., 2006; Pellenard & Deconinck, 2006; Raucsik & Varga, 2008; Dera et al., 2009; Gertsch et al., 2010; Boulila et al., 2022) –see Fig. 7 for synthetic comparison of averaged clay mineral assemblages from the Lower Kimmeridgian in separate areas of Europe and N. Africa). As clay mineral assemblages can largely depend on local factors, regional studies provide a more reliable paleoclimatic signal (Dera et al., 2009) –see Fig. 7. Local forcing mechanisms and climatic changes can thus be disentangled based on the distribution of clay species over time and space, here further discussed in the context of available geochemical and sedimentological data (Coimbra et al., 2014, 2019).

The most landward setting at Rocha Poço has been previously proved to receive a higher original volume of

freshwater along the inner and middle shelf, as interpreted by Coimbra et al. (2014), which agrees with the occurrence of land influence on “coralligenous” facies, even local emersion, across the Algarve Basin (Rosendhal, 1985), with the interpreted 40–50 m depth for sponge buildups (Marques, 1983) in mid-shelf conditions (Ramalho, 1985). Additionally, the silty-to-fine sandy character of the more siliciclastic facies at the base of Rocha Poço allows to assume higher porosity and permeability, in turn promoting a higher water/rock ratio (Coimbra et al., 2014 for full details). Despite previous demonstration that the geochemical record of the carbonate fraction in these facies reflects the influence of meteoric diagenesis, the obtained clay fraction record does not necessarily follow this trend. In fact, several aspects point towards negligible impact of diagenesis in the clay assemblage of the more siliciclastic facies at Rocha Poço: (i) it reveals abundant smectite, a well-known temperature sensitive clay mineral (Arostegui et al., 2006; Boulila et al., 2022) indicating that these deposits have not experienced significant burial –i.e., a corresponding temperature clearly below the 45°C–80°C interval of smectite disappearance (Daoui et al., 2010; Deconinck et al., 2019); (ii) interstratified species as illite/smectite are not dominant along the obtained assemblage, suggesting limited illitization rate and excluding elevated burial temperatures which would severely impact this clay mineral (Środón, 1984), as well as foreseeable higher, comparable values for illite/smectite in the two section analyzed; (iii) the stratigraphic abundance of clay minerals across the siliciclastic interval at Rocha Poço follows the pattern of previously identified terrigenous pulses (Fig. 2), aside from the increased porosity favoring diagenetic alteration. Based on the previous, the stratigraphic distribution of clay species across the siliciclastic interval at Rocha Poço section is considered to reflect depositional conditions (Fig. 7 for wide regional comparison).

As for the remaining facies at Rocha Poço and the Puerto Lorente record, geochemical signatures of the carbonate fraction were previously attributed to the differential influence of forcing mechanisms operating along the south Iberian paleomargin (Coimbra et al., 2014). The potential of preservation of clay species is thus elevated, and again in close agreement with previously identified terrigenous and/or hydrothermal pulses related to tectonic activity resulting in paleomargin structuring (fracture zones and local/regional faults forcing the registered pulses of instability). Clay mineral distribution along both sections is therefore considered to be a suitable proxy for reconstructing regional geodynamic context forcing terrigenous contribution at these areas and related paleoenvironmental conditions at its corresponding hinterlands.

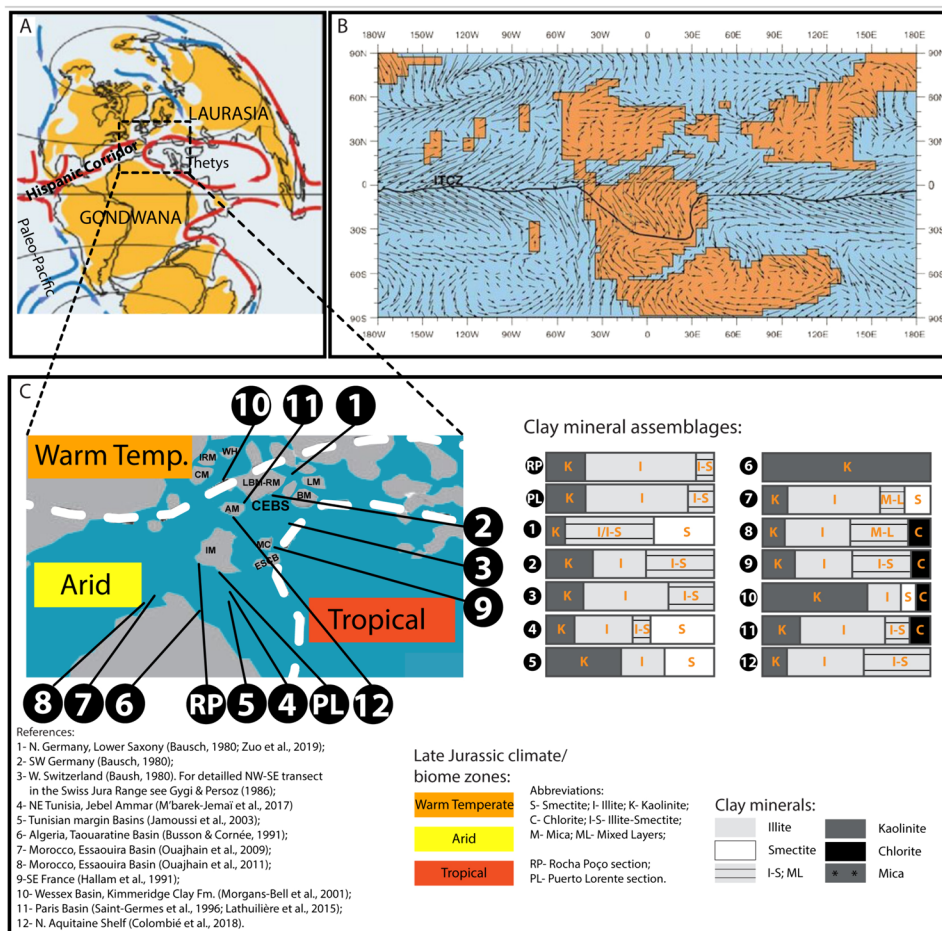


Fig. 7 Paleogeography, climatic zones, global surface currents, global surface winds and averaged composition of clay minerals for early Kimmeridgian times around Iberia. **A** Late Jurassic paleogeography and major sea-surface currents (after Damborenea et al., 2013; red pattern for warm and blue pattern for colder waters). Note that the fragmentation of the Pangea resulted in the development of several marine corridors, among them the Hispanic Corridor and those between Iberia and Africa, affecting oceanic circulation patterns. **B** Simulated surface winds from the Late Jurassic global climate model by Moore et al., (1992a, 1992b). Note that during winter seasons weak-to-moderate northern easterlies would barely affect southern Iberia, while northern Iberia would be affected by moderate northern westerlies and relatively weak storms only during winter, all of this being under the assumption of the low-topography scenario – “500 m plateaus”–modeled by Moore et al., (1992a, 1992b). **C** Synthetic Paleogeography from Kiessling et al. (1999) and Scotese and Wright (2018), combined and modified. *AM* Armorican Massif (Huang et al., 2009). *BM* Bohemian Massif (Colombié, 2002; Kriwet & Klug, 2004; Zuo et al., 2018a, 2018b, 2019). *CEBS* peri-Tethyan Central European Basin System (Pieńkowski & Schudak et al., 2008; Zuo et al., 2019). *CM* Cornubian Massif (Oschmann, 1988; Huang

et al., 2009; Atar et al., 2019). *ESCB* Ebro-Corsican-Sardinian Block (Angrand & Mouthereau, 2021; Nembrini et al., 2021). *IM* Iberian Massif. *IRM* Irish Massif (Pearce et al., 2010; Turner et al., 2018). *LBM-RM-BM* London-Brabant-Rhenish & Boemian Massifs with possibility for at least one seaway between the Rhenish and the Bohemian massifs, with assumed variable depth, in Ziegler, 1992; Brigaud et al., 2008; Thies & Leidner, 2011; Adler, 2013; Hrbek, 2014; Zuo et al., 2018a, 2018b, 2019; Boulila et al., 2022 vs. emerged continuity in between these massifs in Colombié, 2002; Kriwet & Klug, 2004; Pieńkowski & Schudak et al., 2008; Hesselbo et al., 2009; Uhl et al., 2012; Schönlaub, 2016; Turner et al., 2018. Intermittent neritic seaways are here favored (dotted). *LM* Lusitanian Massif (Kriwet & Klug, 2004; Pieńkowski & Schudak et al., 2008; Thies & Leidner, 2011; Zuo et al., 2018a, 2018b). *MC* Massif Central (Boulila et al., 2022). *WH* Welsh High (Turner et al., 2019; Atar et al., 2020). Averaged clay mineral distribution of selected Kimmeridgian case studies distributed around the Iberian Plate, including this work (after Bausch, 1980; Busson & Cornée, 1991; Hallam et al., 1991; Morgans-Bell et al., 2001; Jamoussi et al., 2003; Ouajhain et al., 2009, 2011; Lathuilière et al., 2015; M'barek-Jemai et al., 2017; Colombié et al., 2018; Zuo et al., 2019)

5.2 Mineralogical record and regional paleoenvironmental events

Quartz is present at higher abundance at both sections in correspondence with the events previously identified as

geodynamically active pulses, including pulses of distant, diffusive hydrothermal influence and terrigenous inflow (Figs. 2, 5 and 6). The highest pick of quartz at the Rocha Poço separates two relevant amounts in smectite, and thus probably denotes a tectonic pulse that interrupted a

steady-state pattern of fluctuations in quartz inflows or, alternatively and less probable, a climatic forcing event. High values of quartz at the bottom and middle Puerto Lorente section correlate with tectonic pulses during Platynota chron times under HST (Highstand Systems Tract) conditions. Platynota chron deposits were interpreted as a tectono-eustatic sequence (Olóriz & Rodríguez-Tovar, 1998) starting with a widely recognized instability in western Tethys (Marques et al., 1991). Heterochrony in the second peak of quartz, clearly later in Rocha Poço, seems to reinforce a local forcing effect but at this site could be combined with progradation during Hypselocyclum times under late HST to earliest LST (Lowstand System Tract) conditions. The fact that quartz grains inflows reached both depositional settings attests for their relative proximal position regarding shoreline, allowing to differentiate the Puerto Lorente section as the relatively open (relatively distal?) site in the middle shelf, considering the less significant contribution of quartz at this site (Fig. 6), specially from the mid-section towards the topmost horizons.

Higher combined records of quartz and illite/smectite most probably related to the combination of sea-level rise and tectonic instability (Rocha Poço section), as was identified in the Late Jurassic of the Boulonnais (Hatem et al., 2017). Heterochrony of the noticeable increases of illite/smectite mixed-layers (mid-upper intervals at the Rocha Poço section vs. the lowermost interval at the Puerto Lorente section) reveals changing environmental conditions for deposition and probably early diagenesis, as well as in the tectonic context, through space and time (Godet et al., 2008).

Overall clay mineral contribution supports the previous differentiation among both settings, being more significant at Rocha Poço, a relatively enclosed site in the outer-middle shelf. The fact that the Rocha Poço area was more enclosed when compared to Puerto Lorente is also evident, retaining concomitantly abundant quartz and clay minerals (Fig. 5). Comparatively, at Puerto Lorente, quartz grains become scarcer at the mid-section, whilst clay minerals are overall scarce, to be abundantly recorded only at the topmost portion of the stratigraphic interval, which recorded increasing marly sediments during early mid-Kimmeridgian times under early-HST conditions. This context agrees with the supersequence turnover across Iberia, NW Africa, and the central North Atlantic Basin during early-late Kimmeridgian times, twofold division, (Marques et al., 1991), as well as with starting coarse-up sedimentation and progradation across the western central North Atlantic Basin (Pereira, 2013). Even so, the precise correlation of the respective time resolution scales is at most roughly available, and some diachrony of records could be expected from separated areas.

The isolate increase of illite/smectite and illite in the upmost interval at the Puerto Lorente section is relevant because it is uncoupled with any comparable increase

in clastics (quartz), opposes its usual strong correlation (Gertsch et al., 2010; Boulila et al., 2022), and could inform about smectite transformation in more marly sediments (Godet et al., 2008). Accordingly, a complex intertwined of syn-depositional to post-depositional forcing is envisaged. The dominance of rhythmic deposition of relatively thin marly and limestone couplets accords with the paleoenvironmental trend exposed above, and the lack of concomitant changes in kaolinite content (Šimkevičius et al., 2003) reinforces the role of some diagenetic influence. In fact, the transition from lower to mid-Kimmeridgian deposits coincides with high sea level and occurrence of some diagenetic effect (see Coimbra et al., 2019 for details on diagenesis). This suggests that as sea level rises reaching the aggradation phase (early-to-middle HST), the Puerto Lorente site evolved from a sedimentary bypass area where deposition of terrigenous finer materials was not dominant, towards a relatively more distal depositional zone where under decreasing current energy the presence of clay minerals become more dominant in detriment of quartz, which in turn settles closer to shoreline. This trend accounts for the observed absence of quartz at the topmost levels recording a significant peak of illite and illite/smectite (Fig. 6). Hence, the major increase of illite at the top of this section relates to increase of fine clastics during aggradation-to-initial progradation within HST conditions and the corresponding differential transportation according to floatability; the latter could combine with decreasing chemical weathering (Šimkevičius et al., 2003). Persistence of kaolinite without changes throughout this section is interpreted as a likely climatic signal.

The specific clay species identified in both sections are differentiated, providing a tentative diagnosis of the local paleoclimatic conditions at the respective hinterlands and potential sources of these minerals. Smectite, illite and illite/smectite are the most dominant species at Rocha Poço, with very scarce kaolinite. In contrast, the Puerto Lorente section is characterized by being overall clay-leaner, only showing a prominent illite peak during highest sea-level times.

Smectite and related mixed-layer clays (illite/smectite) are the most abundant clay species throughout the Rocha Poço section, largely following previously identified pulses of diffusive hydrothermal activity (Fig. 2A and 5). Smectite and related interstratified clays are commonly associated to volcanic activity, since it can be found in metaliferous deposits and ash-fall accumulations, both being here absent, or form via submarine weathering of basaltic lava or volcanic sediments and glass (Paquet, 1970; Chamley & Masse, 1975; Singer, 1984; Borchardt, 1989; Chamley, 1989; Cuadros et al., 2011; Duchamp-Alphonse et al., 2011), as well as from tropospheric dusts (Kimblin, 1992; Deconinck & Chamley, 1995). Their favored origin is thus coherent with periods of enhanced volcanic and/or faulting activity in the westernmost Tethys close to the

connection with the growing Hispanic Corridor (Coimbra & Olóriz, 2018). In such a geodynamic context, since the occurrence of volcanic particles, metaliferous deposits and/or hydrothermal vents (chymneis) must be proven, distant venting as well as diffusive hydrothermal influence related to faulting could be responsible for records of pulses of smectite increases. All of this fitting also a scenario of slow erosion rates or erosion of soil horizons formed over long periods of time, to poorly-drained soils and seasonally arid climates (Pearson, 1990; Fürsich et al., 2005). Due to selective sorting, smectite's relatively small size results in preferential deposition in low-energy distal environments. The enclosed nature of the Rocha Poço area accounts for the abundant presence of retained smectite, which allow to consider an alternative (or combined) source. High smectite content (typically > 65%) in clay assemblages is clear evidence of limited burial diagenesis (Boulila et al. (2022), which accords with records in the two sections investigated (Figs. 5 and 6), far from the lowest temperature estimated for smectite withdrawal (Daoudi et al., 2010) and therefore being of detrital origin in a dry and seasonal climate (Godet et al., 2008). Hence, recorded smectite values would indicate deposition of detrital clays under arid/semi-arid and/or seasonal climatic regime at low latitude (Gertsch et al., 2010). Aside from intervals with extremely high values of smectite (lower part at Rocha Poço) probably corresponding to higher aridity and/or erosion (Deconink et al., 2019), smoother standard fluctuations in smectite values most probably relate to rhythmic oscillations of forcing factors (i.e., steady-state conditions of "normal climate"). In contrast, persistent lower but fluctuating values of kaolinite would inform about the overdominance of a low precipitation regime at low latitude with modulated, smoothed, warm temperatures, as well as a constant low biogeochemical weathering, both which resulting from the balancing influence of warm coastal waters of the salty Tethys Ocean (Ross et al., 1992; Godet et al., 2008; Dera et al., 2009; Scotesse & Wright, 2014a, b). Such a smoothed signal precludes hypothetical evidence of a relevant monsoonal influence, supplemented by the NW orientation of the coast. In such a context and given the identified trends in smectite and kaolinite contents, no clear evidence of differential segregation due to respective particle size and floatability contrasts with the expected "normal" behaviour across epicontinental ramps (Chamley, 1989; Raucsik & Merényi, 2000; Godet et al., 2008; Gertsch et al., 2010), such as is well-known in the Late Jurassic of the Boulonnais, SE France (Deconink et al., 1996; Hesselbo et al., 2009).

Illite and related mixed layer minerals (e.g., illite–smectite) can be found particularly in arid and semi-arid regions, where poorly drained areas ensure minimum leaching. Sedimentary records with abundant detrital illite can thus

reflect minimum physico-chemical (and biological) weathering under cold or, in this case, dry climate phases of a mild monsoonal regime, corresponding to low hydrolyzing conditions (Chamley, 1989; Robert & Chamley, 1991), also informing on low degree of diagenetic influence.

Kaolinite is the least abundant clay species recorded throughout both sections (Figs. 5 and 6). Its abundance typically results from the decay of most aluminium silicate parent rocks via highly hydrolytic weathering reactions under warm humid climate (Gaucher, 1981; Chamley, 1989), i.e., humid phases in a monsoonal regime. When scarce in ancient depositional environments, detrital kaolinite indicates low rates of weathering in the hinterland due to low water/rock ratio (Hallam, 1984; Wignall & Ruffell, 1990; Velde, 1992).

In summary, clay mineral species identified at both sections can be attributed to diffusive hydrothermal activity related to faulting at Rocha Poço as well as to overall warm and dry/arid climate conditions accounting for low rates of weathering at the source areas. Based on the above, a Mediterranean-like climate with low runoff is suggested for the area corresponding to the studied sections at the SE Iberia during early Kimmeridgian times, which would be comparatively less humid than interpreted for S. Germany by Uhl et al. (2012).

6 Conclusions

The mineralogical approach applied to previously explored stratigraphic sections provided new and complementary information, including:

- pulses of diffusive hydrothermalism that were identified in all mineralogical components, characterized by abundant quartz provided by nearby areas and equally abundant smectite that can be attributed to local hydrothermal influence coming from fracture zones.
- terrigenous pulses identified both in geochemical and bulk mineralogical data were not very expressive in the clay mineral record, indicating that the Puerto Lorente area was a comparatively bypass area with respect to fine terrigenous materials.
- a conspicuous increase in the clay mineral content towards the topmost horizons of this rhythmic carbonate-siliciclastic deposit as a novel feature, related to a sea-level rising trend and related increase in distality at the Puerto Lorente section.
- Deduced Southern Iberia paleoclimatic conditions are compatible with arid/semi-arid warm climate belt proposed for this region during the Late Jurassic.

Acknowledgements The authors wish to thank Denise Terroso (Dpt. of Geosciences, University of Aveiro) for the support during laboratory procedures. Constructive comments made by two anonymous reviewers and editorial guidance provided by M. Reolid are also acknowledged. This research was supported by Projects CGL2005-01319, CGL2008-05251-E, CGL2010-17629 and CGL2012-39835 (MICINN, MINECO), and the Research Groups RNM-178, Junta de Andalucía, Spain and Geobiotec-UA (UIDB/04035/2020).

Funding Open access funding provided by FCT/IFCCN (b-on).

Data availability Data supporting the findings of this study are available from the corresponding author upon reasonable request.

Declarations

Conflict of interest On behalf of all authors, the corresponding author states that there is no conflict of interest.

Open Access This article is licensed under a Creative Commons Attribution 4.0 International License, which permits use, sharing, adaptation, distribution and reproduction in any medium or format, as long as you give appropriate credit to the original author(s) and the source, provide a link to the Creative Commons licence, and indicate if changes were made. The images or other third party material in this article are included in the article's Creative Commons licence, unless indicated otherwise in a credit line to the material. If material is not included in the article's Creative Commons licence and your intended use is not permitted by statutory regulation or exceeds the permitted use, you will need to obtain permission directly from the copyright holder. To view a copy of this licence, visit <http://creativecommons.org/licenses/by/4.0/>.

References

- Abbink, O., Targarona, J., Brinkhuis, H., & Visscher, H. (2001). Late Jurassic to earliest Cretaceous palaeoclimatic evolution of the southern North Sea. *Global and Planetary Change*, 30(3–4), 231–256.
- Acosta, P. (1989). *Estudio del Jurásico de un sector de la Sierra de Cazorla (Zona Prebética)*, Bachelor Thesis. Univ.
- Adler, L. B. (2013). *The taphonomy of soft-bodied cnidarians* (p. 286). UCD School of Geological Sciences, University College Dublin, Ireland.
- Andrieux, J., Fontboté, J. M., & Mattauer, M. (1971). Sur un modèle explicatif de l'Arc de Gibraltar. *Earth and Planetary Science Letters*, 12, 191–198.
- Angrand, P., & Mouthereau, F. (2021). Evolution of the Alpine orogenic belts in the Western Mediterranean region as resolved by the kinematics of the Europe-Africa diffuse plate boundary. *Bulletin De La Société Géologique De France—Earth Sciences Bulletin*, 192(42), 1–44.
- Arostegui, J., Sangüesa, F. J., Nieto, F., & Uriarte, J. A. (2006). Thermal models and clay diagenesis in the Tertiary-Cretaceous sediments of the Alava block (Basque-Cantabrian basin, Spain). *Clay Minerals*, 41, 791–809.
- Atar, E., Aplin, A. C., Lamoureux-Var, V., März, Ch., & Wagner, Th. (2020). Sedimentation of the Kimmeridge Clay Formation in the Cleveland Basin (Yorkshire, UK). *Minerals*, 10(977), 1–23.
- Atar, E., März, Ch., Aplin, A. C., Dellwig, O., Herringshaw, L. G., Lamoureux-Var, V., Leng, M. J., Schnetger, B., & Wagner, Th. (2019). Dynamic climate-driven controls on the deposition of the Kimmeridge Clay Formation in the Cleveland Basin, Yorkshire, UK. *Climate of the past*, 15, 1581–1601.
- Aurell, M., Meléndez, G., & Bádenas, B. (2002). East Iberian Basins, In *The Geology of Spain*, Geol. Soc. London, edited by W. Gibbons and T. Moreno, Chapter 11- The Jurassic, edited by C.M. Aurell, M. Meléndez and F. Olóriz, pp. 223–235, London, UK.
- Baldy, R., Boillot, G., Dupeuble, P. A., Malod, J., Moita, I., & Mogenot, D. (1977). Carte géologique du plateau continental sud-portugais et sud-espagnol (Golfe de Cadix). *Bulletin De La Société Géologique De France*, XIX, 4, 703–724.
- Bausch, W.M. (1980). Tonmineral provinzen in Malkalken. Erlanger Forschungen Reihe B Naturwissenschaften un Medizin, Band 8, 78 pp.
- Birkeland, Ch. (ed.) (1987). Comparison between Atlantic and Pacific tropical marine coastal ecosystems: community structure, ecological processes, and productivity. Results and scientific papers of a Unesco/COMAR workshop University of the South Pacific Suva, Fiji, 24–29 March 1986. Unesco reports in marine science 46, 99 pp.
- Boillot, G., Dupeuble, P.A., & Mogenot, D. (1974). Géologie du plateau continental portugais entre le cap Carvoeiro et le cap de Sines. *Comptes rendus de l'Académie des Sciences Paris*, 279, serie D, 887–890.
- Borchardt, G.A. (1989). Smectites. In Dixon, J.B. and Weed, S.B. (Eds.), *Minerals in Soil Environments*, 2nd edition. Soil Sci. Soc. America Madison, Wisconsin, pp. 675–727.
- Borges, M. E. N., Riding, J. B., Fernandes, P., & Pereira, Z. (2011). The Jurassic (Pliensbachian to Kimmeridgian) palynology of the Algarve Basin and the Carrapateira outlier, southern Portugal. *Review of Palaeobotany and Palynology*, 163, 190–204.
- Boullin, J. P., Duran-Delga, M., & Olivier, P. (1986). Betic Rifian and Tyrrhenian arc: Distinctive features, genesis and development stages. In F. Wezel (Ed.) *The origin of arcs*. Elsevier, 281–304.
- Boulila, S., Galbrun, B., Gardin, S., & Pellenard, P. (2022). A Jurassic record encodes an analogous Dansgaard-Oeschger climate periodicity. *Nature, Scientific Reports*, 12, 1968.
- Brigaud, B., Pucéat, E., Pellenard, P., Vincent, B., & Joachimski, M. M. (2008). Climatic fluctuations and seasonality during the Late Jurassic (Oxfordian–Early Kimmeridgian) inferred from $\delta^{18}\text{O}$ of Paris Basin oyster shells. *Earth and Planetary Science Letters*, 273, 58–67.
- Brindley, G.W., & Brown, G. (1980). *Crystal Structures of Clay Minerals and their X-Ray Identification*. Mineralogical Society of Great Britain and Ireland, pp. 495.
- Busson, G., & Cornée, A. (1991). The Sahara from the middle Jurassic to the middle Cretaceous: data on environments and climates based on outcrops in the Algerian Sahara. *Journal of African Earth Sciences (and the Middle East)*, 12, 85–105.
- Challinor, A.B., & Hikuroa, D.C.H. (2007). New Middle and Upper Jurassic Belemnite Assemblages from West Antarctica (Latady Group, Ellsworth Land): Taxonomy and Paleobiogeography. *Palaeontologia Electronica*, 10, 1, 6A, 29p.
- Chamley, H. (1989). *Clay Sedimentology* (p. 623). Springer-Verlag.
- Chamley, H., & Masse, J.P. (1975). Sur la signification des minéraux argileux dans les sédiments Barremiens et Bédouliens de Provence. In *Proceedings of the 9th International Sedimentology Congress, Nice, France*, vol. 1, pp. 24–31.
- Chandler, M.A., Rind, D., & Ruedy, R. (1992). Pangean climate during the Early Jurassic: GCM simulations and the sedimentary record of paleoclimate. *Geological Society of American Bulletin*, 104, 543–559.
- Coimbra, R. (2011). Spatial geochemistry and chemostratigraphy across a late Jurassic paleomargin—marine water masses in S-E Iberia. PhD Thesis, GODEL IMPRESIONES, S.L. (ISBN: 978-84-15261-55-1).
- Coimbra, R., Immenhauser, A., Olóriz, F., Rodríguez-Galiano, V., & Chica-Olmo, M. (2015). New insights into geochemical behaviour in ancient marine carbonates (Upper Jurassic Ammonitico

- Rosso): Novel proxies for interpreting sea-level dynamics and palaeoceanography. *Sedimentology*, 62(1), 266–302.
- Coimbra, R., Immenhauser, A., & Olóriz, F. (2014). Spatial geochemistry of Upper Jurassic marine carbonates (Iberian subplate). *Earth Science Reviews*, 139, 1–32.
- Coimbra, R., Kemna, K. B., Rocha, F., & Horikx, M. (2022). Customised display of large mineralogical (XRD) data: Geological advantages and applications. *The Depositional Record*, 8(2), 575–589.
- Coimbra, R., Marques, B., & Olóriz, F. (2019). Testing carbonate chemostratigraphy across differentiated ancient shallow-platform environments (Early Kimmeridgian, S Iberia). *Geoscience Frontiers*, 10, 2203–2218.
- Coimbra, R., & Olóriz, F. (2018). Late Jurassic epicontinental platform dynamics revealed by geochemical patterns of extended deposits (Betic Cordillera, SE Spain). 10th International Congress on the Jurassic System, San Luis Potosí, Mexico, February 2018, Abstracts volume 30.
- Coimbra, R., Rocha, F., Immenhauser, A., Olóriz, F., Terroso, D., & Horikx, M. (2021). Carbonate-hosted clay minerals: A critical re-evaluation of extraction methods and their possible bias on palaeoenvironmental information. *Earth-Science Reviews*, 103502.
- Colombié, C. (2002) Sédimentologie, stratigraphie séquentielle et cyclostratigraphie du Kimméridgien du Jura suisse et du Bassin vocontien (France): relations plate-forme – bassin et facteurs déterminants. PhD 1380, Faculté des Sciences de l'Université de Fribourg, Suisse, 198 pp.
- Colombié, C., Carcel, D., Lécuyer, Ch., Ruffel, A., & Schnyder, J. (2018). Temperature and cyclone frequency in Kimmeridgian Greenhouse period (late Jurassic). *Global Planetary Change*, 170, 126–145.
- Colombié, C., Giraud, F., Schnyder, J., Götz, A. E., Boussaha, M., Aurell, M., & Bádenas, B. (2014). Timing of sea level, tectonics and climate events during the uppermost Oxfordian (Planula Zone) on the Iberian ramp (northeast Spain). *Palaeogeography, Palaeoclimatology, Palaeoecology*, 412, 17–31.
- Comas, M. C., Puga, E., Bargossi, G. M., Morten, L., & Rossi, P. L. (1986). Paleogeography, sedimentation and volcanism of the Central Subbetic Zone, Betic Cordilleras, Southeastern Spain. *Neues Jahrbuch für Geologie und Paläontologie. Monatshefte*, 7, 385–404.
- Cuadros, J., Dekov, V. M., Arroyo, X., & Nieto, F. (2011). Smectite formation in submarine hydrothermal sediments: Samples from the HMS Challenger Expedition (1872–1876). *Clays and Clay Minerals*, 59(2), 147–164.
- Damborenea, S., Echevarría, J., & Ros-Franch, S. (2013). Southern Hemisphere palaeobiogeography of Triassic-Jurassic marine bivalves. Springer, Chapter 1. Introduction. pp. 1–11.
- Daoudi, L., Ouajhain, B., Rocha, F., Rhouta, B., Fagel, N., & Chafiki, D. (2010). Comparative influence of burial depth on the clay mineral assemblage of the Agadir-Essaouira basin (western High Atlas, Morocco). *Clay Minerals*, 45, 453–467.
- Deconinck, J. F., & Chamley, H. (1995). Diversity of smectite origins in Late Cretaceous sediments: Example of chalks from Northern France. *Clay Minerals*, 30, 365–379.
- Deconinck, J. F., Hesselbo, S. P., & Pellenard, P. (2019). Climatic and sea-level control of Jurassic (Pliensbachian) clay mineral sedimentation in the Cardigan Bay Basin, Llanbedr (Mochras Farm) borehole. *Wales. Sedimentology*, 66(7), 2769–2783.
- Deconinck, J. F., Geysant, J. R., Proust, J. N., & Vidier, J. P. (1996). Sédimentologie et biostratigraphie des dépôts kimméridgiens et tithoniens du Boulonnais. *Annales De La Société Géologique Du Nord*, 4, 157–170.
- Demko, T. M., & Parrish, J. T. (1998). Paleoclimatic setting of the Upper Jurassic Morrison Formation. *Modern Geology*, 22, 283–296.
- Dera, D., Brigaud, B., Monna, F., Laffont, R., Pucéat, E., Deconinck, J.-F., Pellenard, P., Joachimski, M. M., & Durlot, C. (2011). Climatic ups and downs in a disturbed Jurassic world. *Geology*, 39(3), 215–218.
- Dera, G., Pellenard, P., Neige, P., Deconinck, J.-F., Pucéat, E., & Domergues, J.-L. (2009). Distribution of clay minerals in Early Jurassic Peritethyan seas: Palaeoclimatic significance inferred from multiproxy comparisons. *Palaeogeography, Palaeoclimatology, Palaeoecology*, 271, 39–51.
- Dercourt, J., Fourcade, E., Cecca, F., Azéma, J., Énay, R., Bassoullet, J.-P., & Cottureau, N. (1994). Palaeoenvironment of the Jurassic system in the Western and Central Tethys (Toarcian, Callovian, Kimmeridgian, Tithonian): An overview. *Geobios*, 17, 625–644.
- Duchamp-Alphonse, S., Fiet, N., Adatte, T., & Pagel, M. (2011). Climate and sea-level variations along the northwestern Tethyan margin during the Valanginian C-isotope excursion: Mineralogical evidence from the Vocontian Basin (SE France). *Palaeogeography, Palaeoclimatology, Palaeoecology*, 302, 243–254.
- Durand-Delga, M., & Fontboté, J. M. (1980). Le cadre structural de la Méditerranée occidentale. 26 Congrès Géologique International, Paris. *Les Chaines alpines issues de la Téthys. Mémoires Du Bureau De Recherches Géologiques Et Minières*, 115, 67–85.
- Fliert, J.R., van de, Hebeda, E.H., Priem, H.N.A., Smet, M.E.M., & Verdurmen, E.A.TH. (1979): Pillow Lavas and basic intrusives of Early Cretaceous age in the Cantar area (prov. Murcia), Spain. *Estudios Geológicos*, 35, 605–608
- Flügel, E. (2010). *Microfacies of Carbonate Rocks, Analysis* (p. 976). Springer-Verlag, Berlin.
- Ford, D., & Golonka, J. (2003). Phanerozoic paleogeography, paleoenvironment and lithofacies maps of the circum-Atlantic margins. *Marine and Petroleum Geology*, 20, 249–285.
- Fürsich, F. T., Singh, I. B., Joachimski, M., Krumm, S., Schlirf, M., & Schlirf, S. (2005). Palaeoclimate reconstructions of the Middle Jurassic of Kachchh (western India): An integrated approach based on palaeoecological, oxygen isotopic, and clay mineralogical data. *Palaeogeography, Palaeoclimatology, Palaeoecology*, 217, 289–309.
- García-Hernández, M., López-Garrido, A. C., Rivas, P., Sanz de Galdeano, C., & Vera, J. A. (1980). Mesozoic palaeogeographic evolution of the External Zones of the Betic Cordillera. *Geologica Mijnbouw*, 59, 155–168.
- Gaucher, G. (1981). Les Facteurs de la Pedogenèse. G. Lelotte, Dison, 730 pp.
- Gertsch, B., Adatte, Th., Keller, G., Tantawy, A.A., Berner, Z., Haydon P. Mort, H.P., & Fleitmann, D. (2010). Middle and late Cenomanian oceanic anoxic events in shallow and deeper shelf environments of western Morocco. *Sedimentology*, 57, 1430–1462
- Godet, A., Bodin, S., Adatte, T., & Follmi, K. B. (2008). Platform-induced clay-mineral fractionation along a northern Tethyan basin-platform transect: Implications for the interpretation of Early Cretaceous climate change (Late Hauterivian-Early Aptian). *Cretaceous Research*, 29, 830–847.
- GTS (2020). Geologic Time Scale 2020. Chapter 26. Jurassic. Hesselbo, S.P., Ogg, J.G., & M. Ruhl, with contributions by Hinnov, L.A., & Huang, C.J. <https://doi.org/10.1016/B978-0-12-824360-2.00026-7>
- Gygi, R. A., & Persoz, F. (1986). Mineralostratigraphy, litho- and biostratigraphy combined in correlation of the Oxfordian (Late Jurassic) formations of the Swiss Jura range. *Eclogae Geologicae Helveticae*, 79(2), 385–454.
- Hallam, A. (1984). Continental humid and arid zones during the Jurassic and Cretaceous. *Palaeogeography, Palaeoclimatology, Palaeoecology*, 47, 195–223.

- Hallam, A., Grose, J. A., & Ruffell, A. (1991). Palaeoclimatic significance of changes in clay mineralogy across the Jurassic–Cretaceous boundary in England and France. *Palaeogeography, Palaeoclimatology, Palaeoecology*, 81, 173–187.
- Hallock, P., & Schlager, W. (1986). Nutrient Excess and the Demise of Coral Reefs and Carbonate Platforms. *Palaios*, 1(4), 389–398.
- Hatem, E., Tribouillard, N., Averbuch, O., BoutRoumazailles, V., Trentesaux, A., Deconinck, J. F., Baudin, F., & Adatte, T. (2017). Small-scaled lateral variations of an organic-rich formation in a ramp-type depositional environment (the Late Jurassic of the Boulonnais, France): Impact of the clastic supply. *Bulletin De La Société Géologique De France*, 188, 31–47.
- Hesselbo, St.P., Deconinck, J.F., Huggett, J.M., & Morgans-Bell, H.S. (2009). Late Jurassic palaeoclimatic change from clay mineralogy and gamma-ray spectrometry of the Kimmeridge Clay, Dorset, UK. *Journal of the Geological Society, London*, 166, 1123–1133.
- Holz, M. (2015). Paleogeografía y paleoclimas mesozoicos: Una discusión sobre las diversas condiciones de invernadero e invernadero de un mundo alienígena. *Journal of South American Earth Sciences*, 61, 91–107.
- Hrbek, J. (2014). The systematics and paleobiogeographic significance of Sub-Boreal and Boreal ammonites (Aulacostephanidae and Cardioceratidae) from the Upper Jurassic of the Bohemian Massif. *Geologica Carpathica*, 65(5), 375–386.
- Huang, Ch., Hesselbo, St.T., & Hinnov, L. (2009). Astrochronology of the late Jurassic Kimmeridge Clay (Dorset, England) and implications for Earth system processes. *Earth and Planetary Science Letters*, 289 (1–2), 245–255.
- Jamoussi, F., Bédir, M., Boukadi, N., Kharbachi, S., Zargouni, F., López-Galindo, A., & Paquet, H. (2003). Clay mineralogical distribution and tectono-eustatic control in the Tunisian margin basins. *Comptes Rendus Geoscience*, 335, 175–183.
- Kiessling, W., Flügel, E., & Golonka, J. (1999). Paleoreef Maps: Evaluation of a Comprehensive Database on Phanerozoic Reefs. *American Association of Petroleum Geologists Bulletin*, 83(10), 1552–1587.
- Kimblin, R. T. (1992). The origin of clay minerals in the Coniacian Chalk of London. *Clay Minerals*, 27, 389–392.
- Kriwet, J., & Klug, St. (2004). Late Jurassic selachians (Chondrichthyes, Elasmobranchii) from southern Germany: Re-evaluation on taxonomy and diversity. *Zitteliana*, A44, 67–95.
- Kriwet, J., & Klug, St. (2008). Diversity and biogeography patterns of Late Jurassic neoselachians (Chondrichthyes: Elasmobranchii). In: Cavin, L., Longbottom, A., & Richter, M. (eds) Fishes and the Break-up of Pangaea. *The Geological Society, London, Special Publications*, 295, 55–70.
- Lanson, B., Sakharov, B. A., Claret, F., & Drits, V. A. (2009). Diagenetic smectite-to-illite transition in clay-rich sediments: A reappraisal of X-ray diffraction results using the multi-specimen method. *American Journal of Science*, 309, 476–516.
- Lathuilière, B., Bartier, D., Bonnemaïson, M., Boullier, A., Carpentier, C., Elie, M., Gaillard, C., Gauthier-Lafaye, F., Grosheny, D., Hantzpergue, P., Hautevelles, Y., Huault, V., Lefort, A., Malartre, F., Mosser, R., Nori, L., Trouiller, A., & Werner, W. (2015). Deciphering the history of climate and sea level in the Kimmeridgian deposits of Bure (eastern Paris Basin). *Palaeogeography, Palaeoclimatology, Palaeoecology*, 433, 20–48.
- Leinfelder, R. (1993). Upper Jurassic reef types and controlling factors. *A Preliminary Report. Profil*, 5, 1–45.
- López-Galindo, A., Olóriz, F., & Rodríguez-Tovar, F.J. (1991). Mineralogical analysis in marly intercalations and integrated approaches to palaeoenvironmental interpretation. An example from the South Iberian margin during the Upper Jurassic. In 7th Euroclay Conference, Proceedings, v. 2, pp. 707–712.
- López-Galindo, A., Olóriz, F., & Rodríguez-Tovar, F. J. (1994). Geochemical traces and sequence stratigraphy analysis during the Upper Jurassic in Southern Iberia. *Mineralogical Magazine*, 58A, 531–532.
- M'barek-Jemaï, M., Sdiri, A., Ben Salah, I., Aissa, L., Bouaziz, S., & Duplay, J. (2017). Geological and technological characterization of the Late Jurassic–Early Cretaceous clay deposits (Jebel Ammar, Northeastern Tunisia) for ceramic industry. *Journal of African Earth Sciences* 129, 282–290.
- Mannupella, G., Marques, B., & Rocha, R. (1988). Evolution tectono-sedimentaire du Bassin de l'Algarve pendant le Jurassique, in 2nd International Symposium of Jurassic Stratigraphy, edited by R.B. Rocha and A.F. Soares, pp. 1031–1046, Lisbon, Portugal.
- Marques, B. (1983). Oxfordiano-Kimmeridgiano do Algarve Oriental: estratigrafia, palaeobiologia (Ammonoidea) e palaeobiogeografia, PhD thesis, Univ. Nova Lisboa, Lisbon, Portugal.
- Marques, B. (1985). Litostratigrafia do Oxfordiano-Kimmeridgiano do Algarve. *Comunicações Dos Serviços Geológicos De Portugal*, 71, 33–39.
- Marques, B., Olóriz, F., & Rodríguez-Tovar, F.J. (1991). Interactions between tectonics and eustasy during the Upper Jurassic and lowermost Cretaceous. Examples from the south of Iberia. *Bulletin de la Société Géologique de France*, 162, 6, 1109–1124.
- Marques, B., & Olóriz, F. (1989a). La marge Sud-Ouest d'Iberie pendant le Jurassique superieur (Oxfordien-Kimmeridgien): Essai de reconstruction geo-biologique. *Cuadernos De Geología Ibérica*, 13, 251–263.
- Marques, B., & Olóriz, F. (1989b). La plate-forme de l'Algarve au Jurassique superieur: Les grandes discontinuités stratigraphiques. *Cuadernos De Geología Ibérica*, 13, 237–249.
- Marques, B., & Olóriz, F. (1992). The *Orthaspidoceras uhlandi* (OPPEL) record and the maximum flooding in the Eastern Algarve during the Lower Kimmeridgian. *Revista Española De Palaeontología, Extra*, 3, 149–156.
- Moore, G. T., Hayashida, D. N., Ross, C. A., & Jacobson, S. R. (1992a). Paleoclimate of the Kimmeridgian/Tithonian (Late Jurassic) world: I. Results using a general circulation model. *Palaeogeography, Palaeoclimatology, Palaeoecology*, 93, 113–150.
- Moore, G. T., Sloan, L. C., Hayashida, D. N., & Umrigar, P. (1992b). Paleoclimate of the Kimmeridgian/Tithonian (Late Jurassic) world: II. Sensitivity tests comparing three different paleotopographic settings. *Palaeogeography, Palaeoclimatology, Palaeoecology*, 95, 229–252.
- Moragues, L., Ruano, P., Azañón, J. M., Garrido, C. J., Hidas, K., & Booth Rea, G. (2021). Two Cenozoic extensional phases in Mallorca and their bearing on the geodynamic evolution of the Western Mediterranean. *Tectonics*, 40, 41pp.
- Morgans-Bell, H.S., Coe, A.L., Hesselbo, St.P., Jenkyns, H.C., Weedon, G.P., Marshall, J.E.A., Tyson, R.V., & Williams, C.J. (2001). Integrated stratigraphy of the Kimmeridge Clay Formation (Upper Jurassic) based on exposures and boreholes in south Dorset, UK. *Geological Magazine*, 138 (5), 511–539.
- Mougenot, D., Monteiro, J. H., Dupeuble, P. A., & Malod, J. A. (1979). La marge continentale sud-portugaise: évolution structurale et sédimentaire. *Ciências da Terra (UNL). Lisboa*, 5, 223–246.
- Nembrini, M., Della Porta, G., & Berra, F. (2021). Development of coral–sponge–microbialite reefs in a coated grain-dominated carbonate ramp (Upper Jurassic, eastern Sardinia, Italy). *Facies*, 67(6), 1–32.
- Olóriz, F. (2002). Betic Cordillera In Aurell, C.M., Meléndez, M., & Olóriz, F. (Eds.), Chapter 11-The Jurassic, 235–237. *The Geology of Spain*, edited by W. Gibbons & T. Moreno. Geological Society of London, London, UK.

- Olóriz, F., & Rodríguez-Tovar, F. J. (1993a). The Oxfordian-Kimmeridgian boundary in the Puerto Lorente section (External prebetic) revisited. *Geogaceta*, *13*, 92–94.
- Olóriz, F., & Rodríguez-Tovar, F.J. (1993b). Lower Kimmeridgian biostratigraphy in the Central Prebetic (Southern Spain. Cazorla and Segura de la Sierra sectors). *Neues Jahrbuch für geologie und Paläontologie. Monatshefte*, 1993 (3), 150–170.
- Olóriz, F., & Rodríguez-Tovar, F. J. (1998). Multifactorial control on deposition of epicontinental hemipelagic carbonates during the earliest Kimmeridgian (Prebetic Zone, southern Spain). *Sedimentary Geology*, *119*, 123–139.
- Olóriz, F., Reolid, M., & Rodríguez-Tovar, F. J. (2003). A Late Jurassic carbonate ramp colonized by sponges and benthic microbial communities (External Prebetic, Southern Spain). *Palaios*, *18*, 528–545.
- Olóriz, F., Reolid, M., & Rodríguez-Tovar, F. J. (2006). Approaching trophic structure in Late Jurassic neritic shelves: A western Tethys example from southern Iberia. *Earth-Science Reviews*, *79*, 101–139.
- Olóriz, F., Reolid, M., & Rodríguez-Tovar, F. J. (2012). Palaeogeography and relative sea-level history forcing eco-sedimentary contexts in Late Jurassic epicontinental shelves (Prebetic Zone, Betic Cordillera): An ecostratigraphic approach. *Earth-Science Reviews*, *111*, 154–178.
- Olóriz, F., Rodríguez-Tovar, F. J., Chica-Olmo, M., & Pardo, E. (1992). The marl-limestone rhythmites from the Lower Kimmeridgian (Platynota Zone) of the central Prebetic and their relationship with variations in orbital parameters. *Earth- Science Reviews*, *111*, 407–424.
- Oschmann, W. (1988). Kimmeridge Clay sedimentation—a new cyclic model. *Palaeogeography, Palaeoclimatology, Palaeoecology*, *65*, 217–251.
- Oujahin, B., Daoudi, L., Laduron, D., Rocha, F., & Naud, J. (2011). Jurassic clay mineral sedimentation control factors in the Essaouira Basin (Western High Atlas, Morocco). *Geologica Belgica*, *14*, 129–142.
- Oujahin, B., Daoudi, L., Medina, F., & Rocha, F. (2009). Contrôle paléogéographique de la sédimentation argileuse du Jurassique du bassin atlasique d'Essaouira (haut atlas occidental, Maroc). *Comunicações Geológicas*, *96*, 51–66.
- Paquet, H. (1970). Evolution géochimique des minéraux argileux dans les altérations et les sols des climats méditerranéens et tropicaux a saisons contrastées. *Mémoires Du Service De La Carte Géologique D'alsace-Lorraine*, *30*, 1–212.
- Parrish, J. T., Ziegler, A. M., & Scotese, C. R. (1982). Rainfall patterns and the distribution of coals and evaporites in the Mesozoic and Cenozoic. *Palaeogeography, Palaeoclimatology, Palaeoecology*, *40*, 67–102.
- Parrish, J.T. (1992). Jurassic Climate and Oceanography of the Pacific Region. In Westermann, G.E.G. (ed.), *The Jurassic of the Circum-Pacific – International Geological Correlation Programme Project 171*, Cambridge University Press p. 365–379.
- Pearce, Ch.R., Coe, A.L., & Cohen, A.S. (2010). Seawater redox variations during the deposition of the Kimmeridge Clay Formation, United Kingdom (Upper Jurassic): Evidence from molybdenum isotopes and trace metal ratios. *Paleoceanography*, *25*, PA4213, <https://doi.org/10.1029/2010PA001963>
- Pearson, M. J. (1990). Clay mineral distribution and provenance in Mesozoic and Tertiary mudrocks of the Moray Firth and northern North Sea. *Clay Minerals*, *25*, 519–541.
- Pellenard, P., & Deconinck, J. F. (2006). Mineralogical variability of Callovo-Oxfordian clays from the Paris Basin and the Subalpine Basin. *Comptes Rendus Geoscience*, *338*, 854–866.
- Pellenard, P., Deconinck, J. F., Huff, W. D., Thierry, J., Marchand, D., Fortwengler, D., & Trouiller, A. (2003). Characterization and correlation of Upper Jurassic (Oxfordian) bentonite deposits in the Paris Basin and the Subalpine Basin, France. *Sedimentology*, *50*, 1035–1060.
- Pendas, E. (1971). Definición morfológica de los embalses subterráneos del alto sureste español. *I Con gr. Hisp.-Luso-Amer. Geol. Econ. Sec. Hidrogeol.*, *II*, 529–550.
- Pereira, R. (2013). Continental rifting and post-breakup evolution of Southwest Iberia: Tectono-stratigraphic record of the first segment of the North Atlantic Ocean. PhD. Thesis, Cardiff University, 343pp.
- Pieńkowski, G., & Schudack, M.E. (co-ordinators) (2008). Jurassic, 101 pp. In: *The Geology of Central Europe*, T. McCann (ed.). Contribution to IGCP project 506 'Marine and Non-marine Jurassic: Global Correlation and Major Geological Events'.
- Rais, P.S.C. (2007). Evidence for a major paleoceanographic reorganization during the Late Jurassic; insights from sedimentology and geochemistry. PhD Thesis. ETH Zurich, 149pp.
- Ramalho, M. (1985). Considerations sur la biostratigraphie du Jurassique superieur de l' Algarve orienlal (Portugal). *Comunicações dos Serviços Geológicos de Portugal*, *71 I*, 4–50.
- Ramalho, M. (1988). Sur la découverte de biohermes stromatolithiques à spongiaires siliceux dans le Kimméridgien de l'Algarve, Portugal. *Comunicações Dos Serviços Geológicos De Portugal*, *74*, 41–55.
- Raucsik, B., & Merényi, L. (2000). Origin and environmental significance of clay minerals in the Lower Jurassic Formations of Mecsek Mts. *Hungary. Acta Geologica Hungarica*, *34*(4), 405–429.
- Raucsik, B., & Varga, A. (2008). Climato-environmental controls on clay mineralogy of the Hettangian-Bajocian successions of the Mecsek Mountains, Hungary: An evidence for extreme continental weathering during the early Toarcian oceanic anoxic event. *Palaeogeography, Palaeoclimatology, Palaeoecology*, *265*, 1–13.
- Rees, P. M., Ziegler, A. M., & Valdes, P. J. (2000). Jurassic phytogeography and climates: New data and model comparisons. In B. T. Huber, K. G. Macleod, & S. L. Wing (Eds.), *Warm climates in earth history* (pp. 297–318). Cambridge University Press.
- Robert, C., & Chamley, H. (1991). Development of early Eocene warm climates as inferred from clay mineral variations in oceanic sediments. *Global and Planetary Change*, *89*, 315–332.
- Rocha, R.B. (1976). Estudo estratigráfico e paleontológico do Jurássico do Algarve ocidental. *Ciências da Terra* *2*, 178 pp.
- Rodríguez-Tovar, F.J. (1993). Evolución sedimentaria y ecostratigráfica en plataformas epicontinentales del margen Sudibérico durante el Kimmeridgiense inferior. PhD Thesis, Universidad de Granada, 374 pp.
- Rosenthal, S. (1985). *Die oberjurassische Korallenfazies von Algarve (Südportugal)* (pp. 82–125). Arbeiten aus dem Institut für Geologie und Paläontologie der Universität Stuttgart.
- Ross, Ch. A., Moore, G. T., & Hayashida, D. N. (1992). Late Jurassic Paleoclimate Simulation-Paleoecological Implications for Ammonoid Provinciality. *Palaios*, *7*, 487–507.
- Ruffell, A., McKinley, J. M., & Worden, R. H. (2002). Comparison of Clay Mineral Stratigraphy to Other Proxy Palaeoclimate Indicators in the Mesozoic of NW Europe. *Philosophical Transactions: Mathematical, Physical and Engineering Sciences*, *360*, 675–693.
- Saint-Germes, M., Baudin, F., Deconinck, J. F., Hantzpergue, P., & Samson, Y. (1996). Sédimentologie de la matière organique et des argiles du Kimméridgien de Normandie (Région du Havre). *Géologie De La France*, *3*, 21–33.
- Schairer, G. (1970). Quantitative Untersuchungen an *Sutneria platynota* (REINECKE) (Perisphinctidae, Ammonoidea) der fränkischen Alb (Bayern). *Mitteilungen der Bayerischen Staatssammlung Für Paläontologie und Historische Geologie, München*, *10*, 153–174.
- Schettino, A., & Turco, E. (2009). Breakup of Pangaea and plate kinematics of the central Atlantic and Atlas regions. *Geophysical Journal International*, *178*, 1078–1097.

- Schnyder, J., Baudin, F., Deconinck, J. F., Durllet, C., Jan du Cène, R., & Lathuilière, B. (2000). Stratigraphie et analyse sédimentologique du passage Oxfordien/Kimmeridgien dans le Boulonnais. *Géologie De La France*, 4, 21–37.
- Schnyder, J., Ruffell, A., Deconinck, J.-F., & Baudin, F. (2006). Conjunctive use of spectral gamma-ray logs and clay mineralogy in defining late Jurassic early Cretaceous palaeoclimate change (Dorset, U.K.). *Palaeogeography, Palaeoclimatology, Palaeoecology*, 229, 303–320.
- Schönlaub, H.P. (2016). Linking geology between the Geoparks Carnic and Karavanke Alps across the Peri-Adriatic Line. In BASE-LiNE Earth (Graz Paleozoic, Geopark Karavanke, Austria), 9–25.
- Scotese, C.R. & Wright, N. (2018). PALEOMAP Paleodigital Elevation Models (PaleoDEMS) for the Phanerozoic PALEOMAP Project. <https://www.earthbyte.org/resource-scotese-and-wright-2018/>.
- Scotese, C.R., & Moore, T.L. (2014b). Atlas of Phanerozoic Ocean Currents and Salinity (Mollweide Projection), Volumes 1–6, PALEOMAP Project PaleoAtlas for ArcGIS, PALEOMAP Project, Evanston, IL., Technical Report, June 2014, 26 pp.
- Scotese, C.R., & Moore, T.L. (2014a). Atlas of Phanerozoic Oceanic Anoxia (Mollweide Projection), Volumes 1–6, PALEOMAP Project PaleoAtlas for ArcGIS, PALEOMAP Project, Evanston, IL.
- Senowbari-Daryan, B., Bucur, I. I., Schlagintweit, F., Săsăran, E., & Matyszkiewicz, J. (2008). *Crescentiella*, a new name for “*Tubiphytes*” *morronei* CRESCENTI, 1969: An enigmatic Jurassic—Cretaceous microfossil. *Geologia Croatica*, 61(2–3), 185–214.
- Šimkevičius, P., Ahlberg, A., & Grigelis, A. (2003). Jurassic smectite and kaolinite trends of the East European Platform: Implications for palaeobathymetry and palaeoclimate. *Terra Nova*, 15(4), 225–229.
- Singer, A. (1984). The paleoclimatic interpretation of clay minerals in sediments. *A Review. Earth-Science Reviews*, 21, 251–293.
- Środoń, J. (1984). Mixed-layer illite-smectite in low-temperature diagenesis: Data from the Miocene of the Carpathian foredeep. *Clay Minerals*, 19, 205–215.
- Stampfli, G. M., & Borel, G. D. (2002). A plate tectonic model for the Palaeozoic and Mesozoic constrained by dynamic plate boundaries and restored synthetic oceanic isochrons. *Earth and Planetary Science Letters*, 196(1–2), 17–33.
- Thierry, J., Abbate, E., Alekseev, A.S., Ait, O.R., Ait, S.H., Bouaziz, S., Canerot, J., Georgiev, G., Guiraud, R., Hirsch, F., Ivanik, M., Le, M.J., Le, N.Y.M., Medina, F., Mouty, M., Nazarevich, B., Nikishin, A.M., Page, K., Panov, D.L., Pique, A., Poisson, A., Sandulescu, M., Sapunov, I.G., Seghedi, A., Soussi, M., Tchoumatchenko, P.V., Vaslet, D., Vishnevskaya, V., Volozh, Y.A., Voznezenski, A., Walley, C.D., Wong, T.E., Ziegler, M., Barrier, E., Bergerat, F., Bracene, R., Brunet, M.F., Cadet, J.P., Guezou, J.C., Jabaloy, A., Lepvrier, C., Rimmele, G., de, W.P., Baudin, F., Belaid, A., Bonneau, M., Coutelle, A., Fekirine, B., Guillocheau, F., Hantzpergue, M., Julien, M., Kokel, F., Lamarche, J., Mami, L., Mansy, J.L., Mascle, G., Pascal, C., Robin, C., Stephenson, R., Sihamdi, N., Vera, J.A., & Vuks, V.J. (2000). Early Kimmeridgian (146–144 Ma). In Peri-Tethys Atlas; Palaeogeographical Maps; Explanatory Notes, Commission for the Geologic Map of the World, Paris, edited by J. Dercourt, M. Gaetani, B. Vrielynck, E. Barrier, B. Biju Duval, M.F. Brunet, J.P. Cadet, S. Crasquin, M. Sandulescu, pp. 85–97.
- Thies, D., & Leidner, A. (2011). Sharks and guitar fishes (Elasmobranchii) from the Late Jurassic of Europe. *Palaeodiversity*, 4, 63–184.
- Thiry, M. (2000). Palaeoclimatic interpretation of clay minerals in marine deposits: An outlook from the continental origin. *Earth-Science Reviews*, 49, 201–221.
- Turner, H.E., Jennifer, M., & Huggett, J.M. (2019). Late Jurassic–Early Cretaceous climate change record in clay minerals of the Norwegian-Greenland Seaway. *Palaeogeography, Palaeoclimatology, Palaeoecology*, 109331, 14pp.
- Turner, H.E., Batenburg, S.J., Gale, A.S., & Gradstein, F.M. (2018) The Kimmeridge Clay Formation (Upper Jurassic–Lower Cretaceous) of the Norwegian Continental Shelf and Dorset, UK: a chemostratigraphic correlation. *Newsletters on Stratigraphy* (pre publ.), 32pp.
- Uhl, D., Jasper, A., & Schweigert, G. (2012). Charcoal in the Late Jurassic (Kimmeridgian) of Western and Central Europe—palaeoclimatic and palaeoenvironmental significance. *Palaeobiodiversity and Palaeoenvironment*, 92, 329–341.
- Valdes, P. J., & Sellwood, B. W. (1992). A palaeoclimate model for the Kimmeridgian. *Palaeogeography, Palaeoclimatology, Palaeoecology*, 95(1–2), 47–72.
- Velde, B. (1992). *Introduction to Clay Minerals* (p. 198). Chapman and Hall.
- Vrielynck, B., & Bouysse, P. (2003). *The Changing Face of the Earth. The Break-up of Pangaea and Continental Drift over the Past 250 Million Years in Ten Steps* (p. 32). CD-ROM included. Commission for the Geological Map of the World.
- Weisser, H., & Mohr, H. (1996). Late Jurassic climate and its impact on carbon cycling. *Palaeogeography, Palaeoclimatology, Palaeoecology*, 122(1–4), 27–43.
- Weissert, H., & Erba, E. (2004). Volcanism, CO₂ and palaeoclimate: A Late Jurassic–Early Cretaceous carbon and oxygen isotope record. *Journal of the Geological Society of London*, 161, 1–8.
- Wierzbowski, A., Atrops, F., Grabowski, J., Hounslow, M.W., Matyja, B.A., Olóriz, F., Page, K.N., Parent, H., Rogov, M.A., Schweigert, G., Villaseñor, A.B., Wierzbowski, H., & Wright, J.K. (2016). Towards a consistent Oxfordian/Kimmeridgian global boundary: current state of knowledge. *Volumina Jurassica*, 14, 15–50.
- Wierzbowski, H., Rogov, M. A., Matyja, B. A., Kiselev, D., & Ippolitov, A. (2013). Middle-Upper Jurassic (Upper Callovian–Lower Kimmeridgian) stable isotope and elemental records of the Russian Platform: Indices of oceanographic and climatic changes. *Global and Planetary Change*, 107, 196–221.
- Wignall, P. B., & Ruffell, A. H. (1990). The influence of a sudden climatic change on marine deposition in the Kimmeridgian of North-West Europe. *Journal of the Geological Society of London*, 147, 365–372.
- Wilkinson, C.R. (1987). Sponge biomass as an indication of reef productivity in two oceans. In Birkeland, Ch. (ed.) Comparison between Atlantic and Pacific tropical marine coastal ecosystems: community structure, ecological processes, and productivity. Results and scientific papers of a Unesco/COMAR workshop University of the South Pacific Suva, Fiji, 24–29 March 1986. Unesco reports in marine science 46, 99–104.
- Wold, S., Esbensen, K., & Geladi, P. (1987). Principal component analysis. *Chemometrics and Intelligent Laboratory Systems*, 2, 37–52.
- Wood, R. (1993). Nutrients, Predation and the History of Reef -Building. *Palaios*, 8, 526–543.
- Wood, R. (1998). The Ecological Evolution of Reefs. *Annual Review of Ecology, Evolution and Systematics*, 29, 179–206.
- Ziegler, A.M., Eshel, G., Rees, McAllister, P., Rothfus, T.A., Rowley, D.B., & Sundelin, D. (2003). Tracing tropics across land and sea: Permian to present. *Lethaia*, 36, 227–254.
- Ziegler, P. A. (1992). North Sea rift system. *Tectonophysics*, 208, 55–75.
- Zuo, F., Heimhofer, U., Huck, St., Addate, Th., Erbacher, J., & Bodin, St. (2019). Climatic fluctuations and seasonality during the Kimmeridgian (Late Jurassic): Stable isotope and clay mineralogical data from the Lower Saxony Basin, Northern Germany. *Palaeogeography, Palaeoclimatology, Palaeoecology*, 517, 1–15.
- Zuo, F., Heimhofer, U., Huck, St., Bodin, St., Erbacher, J., & Bai, H. (2018a). Coupled $\delta^{13}\text{C}$ and $87\text{Sr}/86\text{Sr}$ chemostratigraphy of

Kimmeridgian shoal-water deposits: A new composite record from the Lower Saxony Basin, Germany. *Sedimentary Geology*, 376, 18–31.

Zuo, F., Heimhofer, U., Huck, St., Luppold, F.W., Wings, O., & Erbacher, J. (2018a). Sedimentology and depositional sequences

of a Kimmeridgian carbonate ramp system, Lower Saxony Basin, Northern Germany. *Facies*, 64, 1, 25pp.